Materials Science & Engineering C 114 (2020) 111071

Contents lists available at ScienceDirect

Materials Science & Engineering C

journal homepage: www.elsevier.com/locate/msec

# Magnetosome-anti-*Salmonella* antibody complex based biosensor for the detection of *Salmonella typhimurium*

Sumana Sannigrahi[a], Shiva Kumar Arumugasamy[b], Jayaraman Mathiyarasu[b], Suthindhiran K[a,*]

[a] Marine Biotechnology and Bioproducts Laboratory, School of Bio Sciences and Technology, Vellore Institute of Technology, Vellore 632014, Tamil Nadu, India
[b] Electrodics and Electrocatalysis Division, CSIR - Central Electrochemical Research Institute, Karaikudi 630003, Tamil Nadu, India

ARTICLE INFO

*Keywords:*
Lipopolysaccharide
*Magnetospirillum* sp. RJS1
Magnetosome
ELISA
Electrochemical impedance spectroscopy
*Salmonella typhimurium*

ABSTRACT

Epidemic Salmonellosis contracted through the consumption of contaminated food substances is a global concern. Thus, simple and effective diagnostic methods are needed. Magnetosome-based biosensors are gaining attention because of their promising features. Here, we developed a biosensor employing a magnetosome-anti-*Salmonella* antibody complex to detect lipopolysaccharide (somatic "O" antigen) and *Salmonella typhimurium* in real samples. Magnetosome was extracted from *Magnetospirillum* sp. RJS1 and characterized by microscopy. The magnetosome samples (1 and 2 mg/mL) were directly conjugated to anti-*Salmonella* antibody (0.8–200 μg/mL) and confirmed by spectroscopy and zeta potential. The concentrations of magnetosome, antibody and lipopolysaccharide were optimized by ELISA. The 2 mg/mL-0.8 μg/mL magnetosome-antibody complex was optimal for detecting lipopolysaccharide (0.001 μg/mL). Our assay is a cost-effective (60%) and sensitive (50%) method in detection of lipopolysaccharide. The optimized magnetosome-antibody complex was applied to an electrode surface and stabilized using an external magnetic field. Increased resistance confirmed the detection of lipopolysaccharide (at 0.001–0.1 μg/mL) using impedance spectroscopy. Significantly, the $R^2$ value was 0.960. Then, the developed prototype biosensor was applied to food and water samples. ELISA confirmed the presence of lipopolysaccharide in homogenized infected samples and cross reactivity assays confirmed the specificity of the biosensor. Further, the biosensor showed low detection limit ($10^1$ CFU/mL) in water and milk sample demonstrating its sensitivity. Regression coefficient of 0.974 in water and 0.982 in milk was obtained. The magnetosome-antibody complex captured 90% of the *S. typhimurium* in real samples which was also confirmed in FE-SEM. Thus, the developed biosensor is selective, specific, rapid and sensitive for detection of *S. typhimurium*.

## 1. Introduction

*Salmonella* is one of the most prevalent food pathogens worldwide. Poultry and their eggs, cattle and pigs are infected by *Salmonella*, which can be transmitted to humans by consuming contaminated food [1]. Foodborne diseases caused by *Salmonella* are a major concern in many countries; the World Health Organization (WHO) has estimated that 600,000 deaths occur annually because of typhoid [2], and there are 1.3 billion cases of acute gastroenteritis/diarrhea due to *Salmonella* infection worldwide; leading to 3 million deaths annually [3]. Of these, an estimated 1.4 million occur in developed countries [4]. Recently, 95 isolates of *Salmonella typhi* were reported in the Karnataka region of India [5].

Many of the symptoms of Salmonella infection or Salmonellosis are caused by their characteristic lipopolysaccharide which consists of a major O-antigen with side chains of repeating units of sugar residues [6] and lipid-A which causes the end-stage effects of infection, leading to death in mice, livestock, and humans [7]. The increasing number of Salmonellosis cases has negatively impacted the food industry. Therefore, monitoring food products and maintaining zero counts are essential practices.

Biosensors are promising tools for the detection and monitoring of environmental pollutants and food contaminants that have the unique ability to detect minute quantities of analytes [8–15]. Antibody-based biosensors are currently used to detect various pathogenic microorganisms such as *Escherichia coli*, *Listeria monocytogenes*, *Salmonella typhimurium*, *Campylobacter* sp., *Mycobacterium tuberculosis*, and avian influenza virus [16–23]. Most of these sensors consist of stabilized antibodies attached to the surface of electrodes through physical adsorption or cross-linker molecules [24–27]. However, biomolecule leaching and unwanted analyte crowding on the electrode affect the sensor leading to fluctuations in overall resistance [28,29]. In contrast,

* Corresponding author.
*E-mail address:* ksuthindhiran@vit.ac.in (S. K).

https://doi.org/10.1016/j.msec.2020.111071
Received 9 January 2020; Received in revised form 27 April 2020; Accepted 7 May 2020
Available online 12 May 2020

nanoparticles provide a large specific surface area for catalyzing reactions [30,31] which improves the performance of the biosensor [32–37]. However, the varied size range and linkers used to immobilize nanoparticles on the electrode surface introduces complexity into the process and affects the binding kinetics [38–42].

To overcome these problems, we propose the use of magnetosome-based biosensors for the detection of *Salmonella*. The magnetosome is a biogenic nanoparticle, 35–120 nm size, which is synthesized in few genus of *Magnetospirillum* sp. of magnetotactic bacteria through biomineralization [43,44]. Compared to other nanoparticles, magnetosome have a narrow, uniform size range, strong ferromagnetic behavior and regular crystallographic features [45,46]. Magnetosome have a unique lipid bilayer membrane consisting of phospholipids and phosphatidylethanolamine [47,48]. These provide an outward amine group, which is biocompatible for conjugation with biological entities [49,50]. In previous reports, the electrode surface was often coated with a chemically synthesized bilayer lipid membrane (BLM), because it acts as a signal transducer and a bipolar electrode for antibody-antigen reactions [18,51]. Since, the magnetosome has a biologically synthesized lipid bilayer on its surface, it can be directly used in antibody-based biosensors. Magnetosome have superior dispersion and handling properties compared to conventional $Fe_3O_4$ nanoparticle which lacks lipid bilayer membrane [52–54]. The magnetic nature of the magnetosome allows the antibody to be stabilized on the electrode surface by an external magnet, thereby simplifying the process. Wu et al. [55] developed magnetosome based immunosensor for detection of enterotoxin in milk. The sensor was rapid but the process was costly and complex due to the use of gold electrodes.

The present study describes the direct conjugation of magnetosome with anti-*Salmonella* antibody and the detection of *Salmonella* lipopolysaccharide using a screen-printed carbon electrode (SPCE). Further, the biosensor detects *S. typhimurium* in water and milk samples.

## 2. Reagents and chemicals

The primary antibody (rabbit polyclonal antibody against *Salmonella* [anti-*Salmonella* antibody]) was purchased from Abcam (ab35156; India), and the secondary antibody (goat anti-rabbit IgG conjugated to horseradish peroxidase [HRP]) was purchased from GeNei™ Products (621140380011730; Merck India, Biosciences). Lipopolysaccharide from *Salmonella enterica* serotype *typhimurium* purified by trichloroacetic acid extraction was purchased from Sigma (L7261; India). SPCE (SPCE DRP-110) was purchased from DropSens (Spain). *S. typhimurium* (MTCC-98) was purchased from Microbial Type Culture Collection and Gene Bank (MTCC, India) and maintained in Nutrient agar. Bovine serum albumin (BSA), potassium ortho phosphate ($KH_2PO_4$), sodium nitrate ($NaNO_3$), sodium thioglycolate ($HSCH_2COONa$), L(+) tartaric acid (extra pure), sodium acetate ($C_2H_3O_2Na$), sodium chloride, potassium chloride, di-sodium hydrogen phosphate dehydrate, potassium di hydrogen phosphate, tris, anhydrous sodium carbonate, sodium bicarbonate, tween-20, citric acid, dibasic sodium phosphate, potassium ferrocyanide ($K_4[Fe(CN)_6]$), potassium ferrocyanide ($K_3[Fe(CN)_6]$) and MacConkey agar were purchased from Himedia Laboratories (India). 2,2-Azino-bis (3-ethylbenzothiazoline-6-sulfonic acid) diammonium Salt (ABTS [extrapure AR 98.5%]), succinic acid (extra pure), ferric citrate, quinic acid, and 0.1% resazurin were purchased from Sisco Research Laboratories (India). Hydrogen peroxide (30% w/v) was purchased from Spectrum Reagents and Chemicals (India).

### 2.1. Extraction and characterization of the magnetosome

*Magnetospirillum* sp. RJS1 [56] was cultured in *Magnetospirillum* growth media (MSGM) using the Hungate anaerobic technique [57,58]. Bacterial growth and magnetosome production were monitored at regular intervals by placing the culture bottle on a magnetic stirrer [59]. Magnetosome was lyophilized (Lark, Penguin Classic Plus, India) and characterized through Field Emission Scanning Electron Microscopy (FESEM) and Transmission Electron Microscopy (TEM) and Energy-dispersive X-ray spectroscopy (EDS). To analyse the morphology, size range and purity of extracted magnetosome, FESEM (Zeiss EV018, Germany operating at 10kv) TEM (HR-TEM, JEOL JEM2100, Japan operating at 200kv) and EDS (BrukerEasy) analysis was performed. Magnetosome was dispersed in distilled water and drop casted on slides, incubated for overnight and viewed under FESEM. TEM analysis was done by directly dropping the dispersed magnetosome on the copper grid and viewed. Powdered magnetosomes was placed on glass slide for EDS analysis.

### 2.2. Functionalization of magnetosome with anti-Salmonella antibody

Magnetosome was bound to anti-*Salmonella* antibody by using a modified protocol adapted from Woo et al. [60]. Briefly, two magnetosome stocks (1 and 2 mg/mL) were prepared in phosphate buffered saline (PBS) in tubes. The tubes were placed one by one under the probe in the sonicator (VCX-130W-220VAC-VIBRA-CELL SYSTEM; Sonics & Materials, USA) in 35 kHz frequency at 30 W for 5 min. Once the sonication was done, dispersed magnetosome solution was collected. For functionalization, antibody (100 μL of 200 μg/mL) was added to 900 μL of dispersed magnetosome solution and incubated at 4 °C for 24 h. The magnetosome-antibody complex was collected with a neodymium magnet and washed with PBS containing 1% BSA for 10–12 times to remove unbound antibodies. The absorbance of the magnetosome-antibody complex was measured at 630 nm with a 96- well plate reader (LIMR96; Lark Innovative Fine Teknowledge, India) and compared with that of the controls (i.e., magnetosome and antibody separately). Other concentrations of antibodies (0.8–40 μg/mL) were prepared by diluting in PBS.

Electrochemical Impendence Spectroscopy (EIS) was used to determine the coupling of magnetosome with anti-*Salmonella* antibody [61]. The disposable SPCE consisted of a carbon working electrode, carbon counter electrode and silver reference electrode. A series of SPCE's were obtained, and the bare response was measured. Then, 10 μL of anti-*Salmonella* antibody (0.8 μg/mL) was applied to the working electrode. A bar magnet was placed beneath the SPCE and incubated at 37 °C for 30 min. The SPCE was rinsed continuously with PBS buffer for 30 s and then immersed twice in deionized water. Next, 10 μL of magnetosome (2 mg/mL) was applied to the working electrode and incubated at 37 °C for 60 min. Finally, the SPCE was immersed in PBS for 30 s and washed twice with deionized water. EIS measurements were acquired in an open circuit, with a potential of 0.13 V using an electrolyte containing 2.5 mM $K_4[Fe(CN)_6]$, 2.5 mM $K_3[Fe(CN)_6]$ and 0.1 M KCl prepared in 10 mM PBS (pH 7.4). Nyquist diagrams were recorded of imaginary impedance vs. real impedance from 0.1 Hz to 100 kHz, with an amplitude of 5 mV. A fitting spectrum was generated from the data using ZVIEW software. The impedance responses at various concentrations (0.8–200 μg/mL) of anti-*Salmonella* antibody and magnetosome-anti-*Salmonella* antibody complex were similarly measured.

Fourier-transform infrared spectroscopy (FTIR) analysis was done to determine the binding of magnetosome with antibody. The powdered magnetosome, anti-*Salmonella* antibody and magnetosome-anti-*Salmonella* antibody complex were directly analysed in FTIR spectrophotometer (Schimadzu, Japan) between 400 $cm^{-1}$ and 4000 $cm^{-1}$ wavelength.

Zeta potential (Horiba Scientific SZ-100) analysis was done to determine the electrostatic interaction between magnetosome and antibody.

### 2.3. Screening of Salmonella typhimurium (ATCC-7823) lipopolysaccharides

#### 2.3.1. Attachment of lipopolysaccharides to the magnetosome-anti-Salmonella antibody complex

Carbonate-bicarbonate buffer was prepared according to a standard protocol as follows: 20 mL of sodium carbonate solution was added to 225 mL of sodium bicarbonate solution and 1000 mL of distilled water. A lipopolysaccharide stock (0.01 μg/mL) was prepared in the carbonate-bicarbonate buffer (pH 9.2). Then, 100 μL of the lipopolysaccharide stock was loaded into 96 well plates and incubated at 4 °C overnight. The coated wells were washed thrice with PBS-Tween 20 (PBST) and incubated at room temperature for 5 min. The process was repeated, and 100 μL of the magnetosome (1 or 2 mg/mL)-anti-*Salmonella* antibody (0.8–200 μg/mL) complex was loaded into the washed wells. The plate was incubated at 37 °C for 60 min. The magnetosome-antibody-lipopolysaccharide complex was congregated on the plate using a magnet. Unbound antibodies were removed by washing thrice with PBST, and the absorbance was measured at 630 nm.

#### 2.3.2. ELISA using the magnetosome-anti-Salmonella antibody complexes to detect lipopolysaccharide

The magnetosome (1 or 2 mg/mL)-anti-*Salmonella* antibody complexes were used, along with an HRP-conjugated secondary antibody, to detect the presence of lipopolysaccharide by ELISA. Wells were coated with 100 μL of lipopolysaccharide (0.001 μg/mL) as described above. Next, 100 μL aliquots of various concentrations of magnetosome-antibody complexes (0.8–200 μg/mL) were added to the wells and then washed to remove unbound magnetosome-antibody complexes. A control without magnetosome i.e. antibody alone was also included. Then, a 100 μL aliquot of the HRP-conjugated secondary antibody (0.2 μg/mL) was added to the wells and incubated at room temperature for 60 min. The lipopolysaccharide-magnetosome-anti-*Salmonella* antibody-secondary antibody complex was collected with an external magnet and washed with PBST three times to remove unbound secondary antibody. 100 μL of ABTS substrate was added to the wells and after a 30 min incubation, the absorbance was measured at 405 nm with a plate reader.

ELISA using the magnetosome-antibody complex (with 1 or 2 mg/mL magnetosome) was performed to determine the minimum detectable concentration of lipopolysaccharide. The wells of a 96-well plate were coated with 100 μL aliquots of 0.001–5 μg/mL lipopolysaccharide. Then, a 100 μL sample of magnetosome–antibody complex (4 μg/mL) and HRP-conjugated secondary antibody (0.2 μg/mL) were loaded into the lipopolysaccharide-coated wells, and the remaining process was performed as described above.

### 2.4. EIS to detect lipopolysaccharide

The interaction of the magnetosome (2 mg/mL)-antibody complex with lipopolysaccharide was also studied by EIS. A series of magnetosome-antibody (0.8 μg/mL) complex fabricated SPCE's were used. A 15 μL sample of lipopolysaccharide (0.01 μg/mL) was applied to the fabricated SPCE's and incubated at 37 °C for 60 min. The electrode was then rinsed twice with PBS and deionized water. The impedance responses for lipopolysaccharide were measured using PARSTAT (Princeton Applied Research) electrochemical workstation. Similarly, the interactions of magnetosome (2 mg/mL)-antibody (0.8 μg/mL) complex with other concentrations of lipopolysaccharide (0.1, 0.05, 0.01, 0.005 and 0.001 μg/mL) were also studied.

### 2.5. Detection of lipopolysaccharide extracted from infected samples and a cross-reactivity assay

The detection protocol was modified from Varshney et al. [62]. Briefly, water sample and milk samples were inoculated with *S. typhimurium* in separate tubes and incubated at 37 °C for 24 h in an orbital shaker at 120 rpm and continuously monitored. Once growth was observed, the samples were transferred to centrifuge tubes. They were homogenized for 10 min and then centrifuged at 1000 $\times g$ for another 10 min to separate the cells from the solid food particles and cell debris. The homogenized samples were loaded into 96-well plates, which were coated with buffer and incubated overnight at 4 °C. ELISA was performed using anti-*Salmonella* antibody (0.8 μg/mL) alone as well as magnetosome-antibody complex (2 mg/mL-0.8 μg/mL). EIS of the *Salmonella*-infected homogenized milk and water samples was also performed. Homogenized samples were added to the magnetosome-antibody complex at a ratio of 1:1 and incubated at 37 °C for 30 min. A bar magnet was attached to the tube, and the tube was washed twice with distilled water. A 10 μL sample was placed on the SPCE, and the impedance was measured using a solution containing 2.5 mM $K_4[Fe(CN)_6]$ and, 2.5 mM $K_3[Fe(CN)_6]$. A cross-reactivity assay was also performed to check the sensitivity and specificity of the magnetosome-antibody (2 mg/mL-0.8 μg/mL) complex with respect to other pathogens. In this test, milk samples were inoculated with four different pathogens: *S. typhimurium* (MTCC 98), *E. coli* (MTCC 1687), *L. monocytogenes* (MTCC 657), and *S. aureus* (MTCC 1144) in separate tubes. Homogenized samples for each pathogen were obtained and EIS was conducted using the magnetosome-antibody complex.

### 2.6. Sensitivity and capture efficiency assays

The protocol used for this experiment was a modification of Varshney and Li [63]; Setterington and Alocilja [64], and Sheikhzadeh et al. [65]. The overnight culture (*S. typhimurium*) was taken and centrifuged at 1000 $\times g$ for 5 min. The bacterial pellet was washed continuously and resuspended in PBS buffer. The initial concentration of bacteria was calculated and further diluted to maintain $10^7$ CFU/mL. Water and milk samples (900 μL) were placed in separate tubes and a 100 μL aliquot of $10^7$ CFU/mL was added to both tubes. Serial dilutions ($10^1$–$10^7$ CFU/mL) of the water and milk samples were prepared using a standard protocol. A 100 μL sample of magnetosome-antibody complex (2 mg/mL-0.8 μg/mL) was added to 100 μL of the cells (serially diluted in water or milk). Then, the tubes were incubated at 37 °C for 30 min in an orbital shaker. A bar magnet was attached to the tube, and the content was washed twice with distilled water. The magnetosome-antibody-*S. typhimurium* complex (water/milk sample) (10 μL) was placed on the SPCE, and impedance was measured. A set of controls (milk/water samples without *S. typhimurium*) was mixed with the magnetosome-antibody complex, and impedance was measured. The FE-SEM analysis was carried out to confirm the interaction of magnetosome-antibody complex with *S. typhimurium* in milk sample. Briefly, magnetosome-antibody-*S. typhimurium* complex was collected from test sample (milk, $10^4$ CFU/mL). The complex was then placed on clean silicon sheet. After 30 min, 0.25% of glutaraldehyde was added over the dried complex and incubated at 4 °C for 12 h. The sheet was collected after the incubation, and the complex was continuously dehydrated at room temperature using various concentrations (70, 80, 90 and 100%) of ethanol. The sheet containing the complex was then viewed under the electron microscope. A capture efficiency assay was performed to determine the number of *S. typhimurium* captured from the water and milk samples by the magnetosome-antibody complex. The magnetosome-antibody complex conjugated with *Salmonella* ($10^1$, $10^2$, $10^3$, $10^5$, and $10^7$ CFU/mL) was plated on MacConkey agar. Controls ($10^1$, $10^2$, $10^3$, $10^5$, and $10^7$ CFU/mL) containing pure culture in water or milk sample were also platted (Scheme 1).

$$\text{Capture efficiency} = \text{Number of viable cells captured} \Big/ \text{Number of viable cells in an original dilution} \times 100 \quad (1)$$

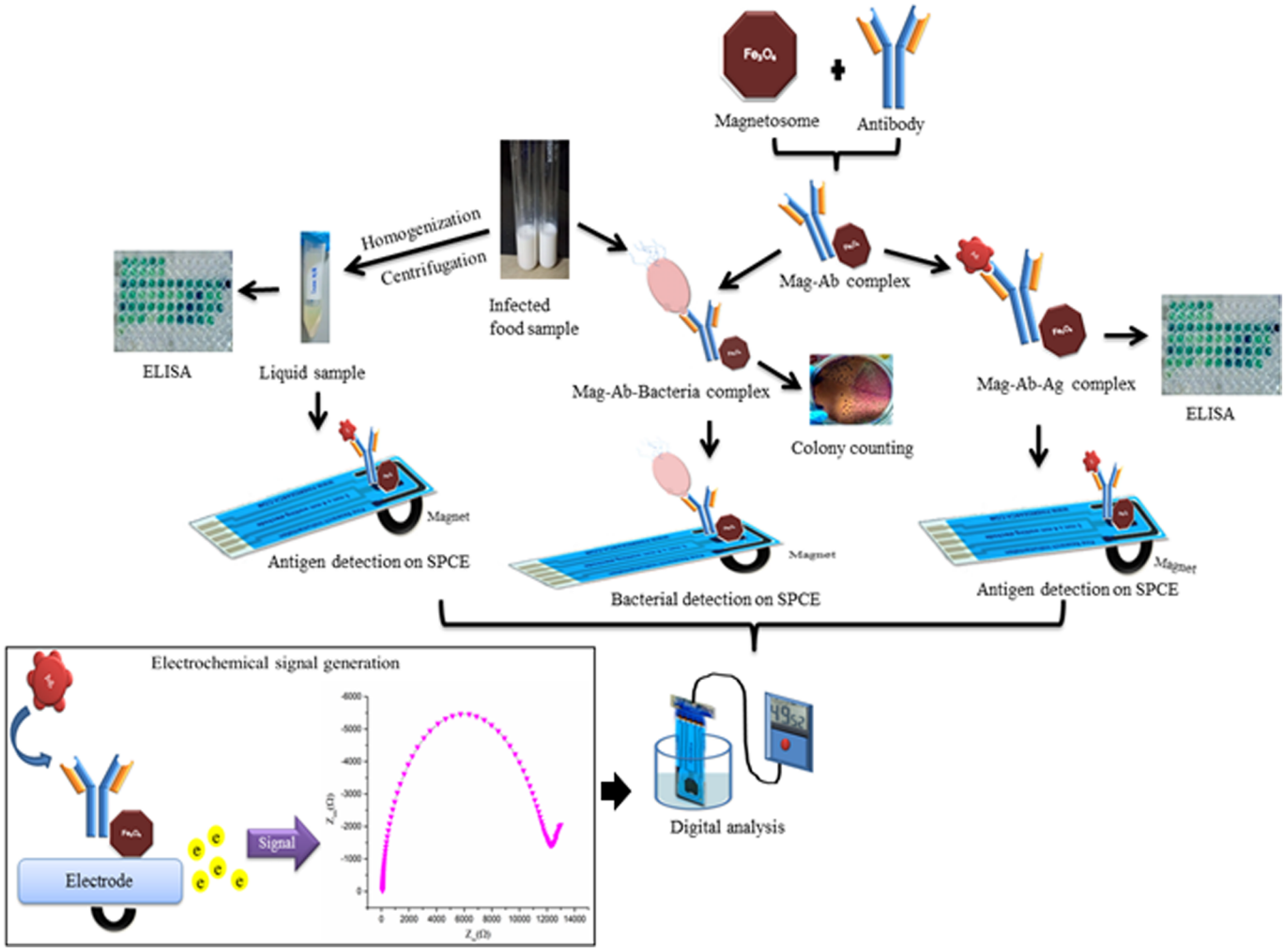


**Scheme 1.** Schematic illustration of lipopolysaccharide and *Salmonella typhimurium* detection using magnetosome-anti-*Salmonella* antibody complex.

## 3. Results

### 3.1. Extraction and characterization of the magnetosomes

Magnetosome was extracted from *Magnetospirillum* sp. RJS-1 which yielded 4–6 mg of magnetosome per 1 L of culture. FE-SEM confirmed that magnetosome was in the nano-size range (Fig. 1A) and uniform size distribution. TEM demonstrated the cubo-octahedral shape of magnetosome (Fig. 1B). The EDS analysis showed that magnetosome contain iron in it, which represents, they belong to magnetite (Fig. 1C).

### 3.2. ELISA for detecting lipopolysaccharide without magnetosomes

An ELISA was performed to detect lipopolysaccharide using different concentrations of lipopolysaccharide (0.01–5 μg/mL), anti-*Salmonella* antibody (0.08–200 μg/mL) and HRP-conjugated secondary antibody (0.1–1 μg/mL). For lipopolysaccharide, 0.01 μg/mL was selected as the standard concentration. The concentrations of anti-*Salmonella* antibody and HRP-conjugated secondary antibodies were optimized and determined to be 4 and 0.2 μg/mL, respectively (Fig. S1).

### 3.3. Binding of magnetosome to anti-Salmonella antibodies

Conjugation of the anti-*Salmonella* antibody with magnetosome was confirmed by the absorbance spectra. For 1 mg/mL magnetosome, the average absorbance of the magnetosome-antibody complex (0.214) was higher than that of magnetosome (0.171) or antibody alone 0.104 (Fig. S2A). Similarly, at 2 mg/mL magnetosome, the average absorbance of the magnetosome-antibody complex (0.248) was higher than magnetosome (0.191) or antibody alone (0.104; Fig. S2B). The difference in the absorbance of the complex compared to the components alone confirmed magnetosome antibody binding.

EIS was performed with the 2 mg/mL stock of magnetosome because the conjugate showed higher absorbance. The bare carbon electrode exhibited an $R_{CT}$ value of 285 Ω, whereas the antibody (0.8 μg/mL)-coated electrode showed a two-fold increase ($R_{CT}$ = 564 Ω; Fig. 2A, Table S1). The $R_{CT}$ value of the magnetosome was 978 Ω, and that of the magnetosome-antibody (0.8 μg/mL) complex was 1202 Ω. As the $R_{CT}$ value of the magnetosome-antibody complex was higher than the magnetosome only and two-fold higher than the antibody only, this indicated that the magnetosome effectively coupled with the antibody (Fig. 2A, Table S1).

EIS was performed at different concentrations of anti-*Salmonella* antibody (0.8–200 μg/mL) and magnetosome-anti-*Salmonella* antibody (0.8–200 μg/mL) complex. The highest concentration of antibody (200 μg/mL) showed a $R_{CT}$ value of 2064 Ω, which was higher than the $R_{CT}$ values at the lower concentrations, which were 1468, 996, 852, and 591 Ω at 40, 4, 1.6, and 0.8 μg/mL, respectively (Fig. 2B, Table S2), demonstrating a decrease in $R_{CT}$ value with decreasing antibody concentration. The magnetosome-antibody complex at 200 μg/mL exhibited a high $R_{CT}$ value of 4154 Ω, whereas the values at 40 and 4 μg/mL were 3295 and 2082 Ω, respectively (Fig. 2C, Table S3) and the values at 1.6 and 0.8 μg/mL were 1492 and 1184 Ω, respectively. The calibration graphs (Fig. 2B and C) clearly show a linear relationship

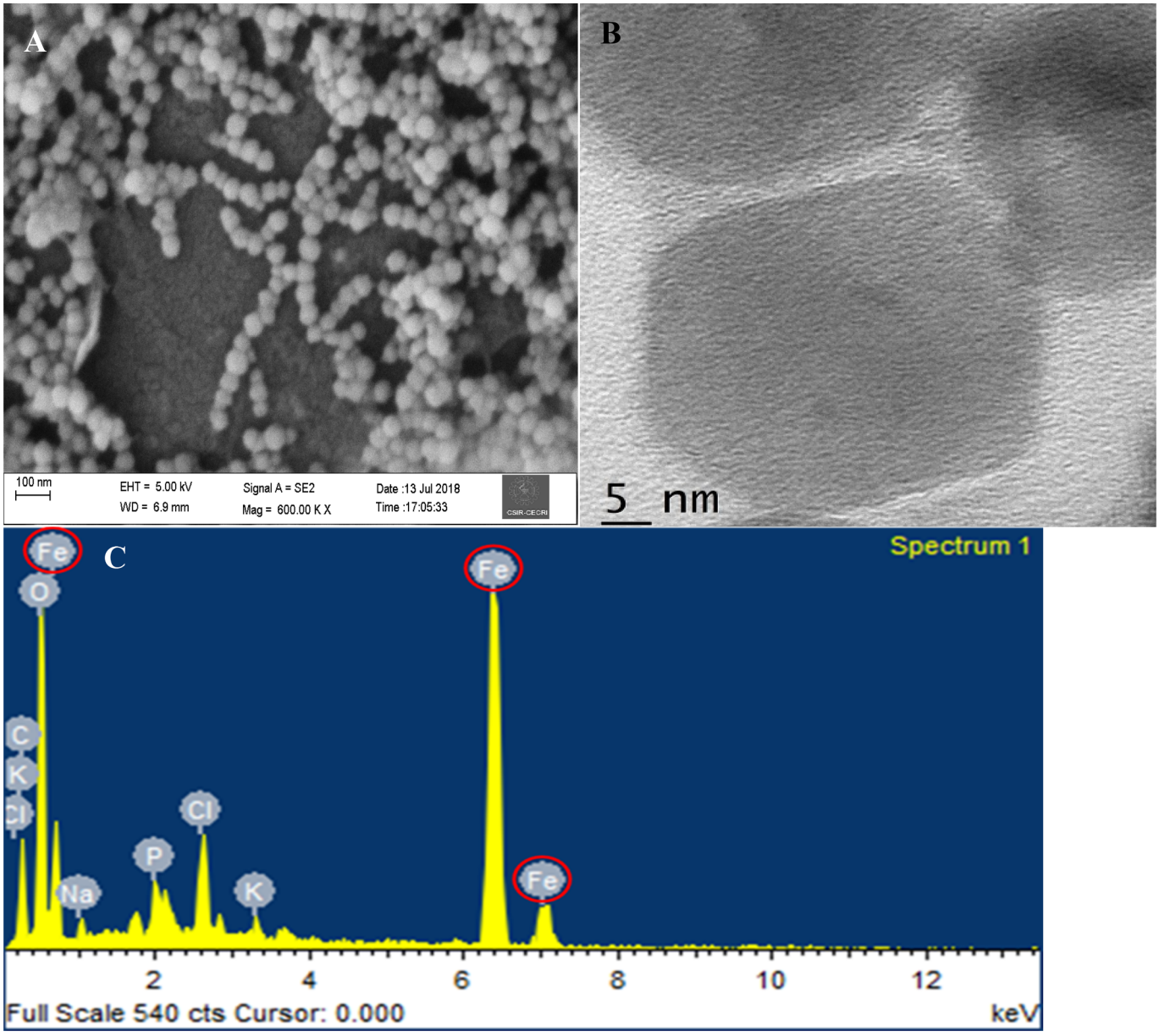


**Fig. 1.** (A): FE-SEM image showed the uniform morphology of magnetosomes at 100 nm scale bar. (B) TEM image showed the cubo-octahedral shape of magnetosomes at 5 nm scale bar. (C) EDS analysis of magnetosomes confirms the presence of iron.

between concentration and $R_{CT}$ value, with a regression coefficients of 0.984 and 0.991. Thus, the higher the concentration of antibody, the higher the resistance was obtained.

FTIR analysis of antibody showed two stretches at 3221.12 $cm^{-1}$ for O—H bond and 1649.14 $cm^{-1}$ for N—H bond representing the α helix structure of the protein. A dominant peak at 1062.78 $cm^{-1}$ represents the C—N bond of amide I in proteins and 981.77 $cm^{-1}$ for amide IV. The peak at 852.54 $cm^{-1}$ shows hydrogen bonding while the peak at 611.43 $cm^{-1}$ represents amide IV with O = C–N deformation. The peak at 518.85 $cm^{-1}$ shows amide VI bonds (Fig. 2D).

FTIR analysis of magnetosome showed stretches at 3273.20 $cm^{-1}$ for O—H bond, 3076.45 $cm^{-1}$ and 3028.24 $cm^{-1}$ representing C—H bond for unsaturated fatty acids. Stretches at 2924.09 $cm^{-1}$, 2852.72 $cm^{-1}$ and 1462 $cm^{-1}$ for C—H bond, 1629.80 $cm^{-1}$ and 528.50 $cm^{-1}$ for Fe—O bond, 1047.35 $cm^{-1}$ for C═O bond and 2852.72 $cm^{-1}$ representing methylene group in membrane lipids were also observed in FTIR spectrum of magnetosome (Fig. 2D). Fe—O bond represents the magnetic nature of the magnetosome. Amide vibration was evident in 1525.69 $cm^{-1}$ wavelength. Stretches at 1402.26 $cm^{-1}$ showed the presence of C = O-lipids while 864.11 $cm^{-1}$ showed C═O and C—C vibration.

The successful binding of antibody on the surface of magnetosome can be confirmed by FTIR analysis. There was a shift in stretching vibration from 3273.20 $cm^{-1}$ to 3278.99 $cm^{-1}$ in magnetosome-antibody complex depicting the formation of amide A bonds. The additional peak at 2958.80 $cm^{-1}$ showing the C—H vibration was also observed. The prominent stretches at 1643.36 $cm^{-1}$ (C═O stretch) and 1535.34 $cm^{-1}$ (N—H bend with C—N stretch) representing amide I and amide II respectively were present in addition to 1242.16 $cm^{-1}$, 1076.28 $cm^{-1}$ and 987.55 $cm^{-1}$. This might be due to the covalent attachment of magnetosome to the amine-terminated surface of antibody. Upon attachment of antibody on the surface of magnetosome, few additional peaks 1454.33 $cm^{-1}$ representing $CH_2$ and 1398.39 $cm^{-1}$ representing carbonyl groups were observed.

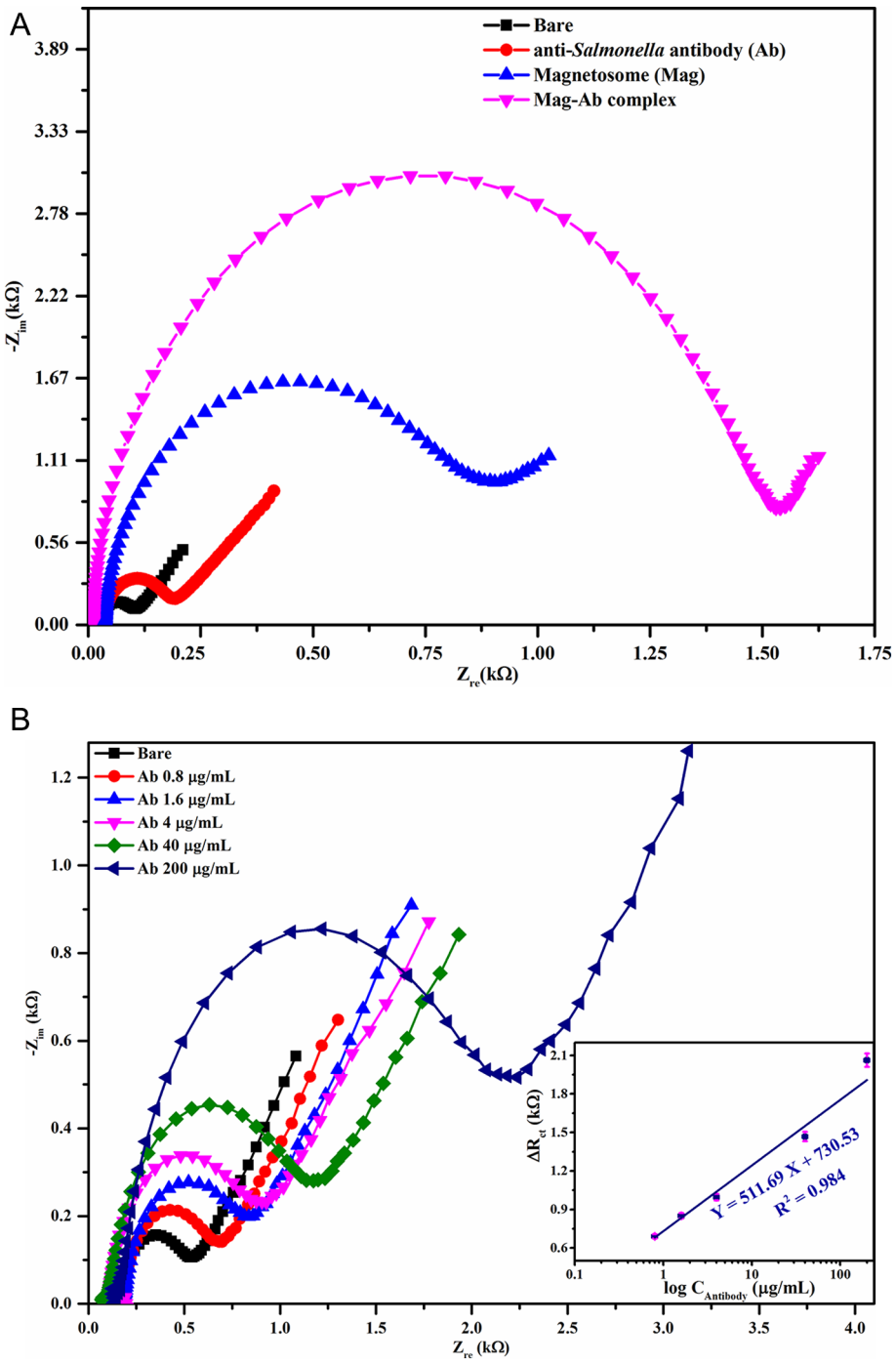


**Fig. 2.** (A): Nyquist plot obtained for the interaction of anti-*Salmonella* antibody (0.8 μg/mL) with magnetosome (2 mg/mL).
(B): Nyquist plot obtained for various concentrations of anti-*Salmonella* antibody (0.8–200 μg/mL) with a calibration plot of $\Delta R_{ct}$ with log ($C_{Antibody}$).
(C): Nyquist plot obtained for various concentrations of magnetosome-anti-*Salmonella* antibody complex (0.8–200 μg/mL) with a calibration plot of $\Delta R_{ct}$ with log ($C_{Mag\text{-}Antibody}$).
(D): FTIR analysis of antibody, magnetosome and magnetosome-antibody complex.

Zeta potential of magnetosome was negative (−14.4 mV) due to the negative groups present in the lipid bilayer membrane. The antibody, on the other hand, showed similar zeta potential (−14.6 mV) confirming its stable nature. However, the coupling of magnetosome to antibody increased the zeta potential value (−17.3 mV). The increase in zeta potential value proved magnetosome-antibody complex to be more stable than the unconjugated ones.

### *3.4. Screening of lipopolysaccharides with magnetosome-antibody complex*

#### *3.4.1. Attachment of lipopolysaccharides with magnetosome-anti-Salmonella antibody complexes*

The interaction of magnetosome (1 or 2 mg/mL)-anti-*Salmonella* antibody complexes with lipopolysaccharide was evaluated. The absorbance of the magnetosome (1 mg/mL)-antibody (200 μg/mL) with lipopolysaccharide (0.294) was higher than the absorbance of the magnetosome-antibody (200 μg/mL) complex alone (0.264) and

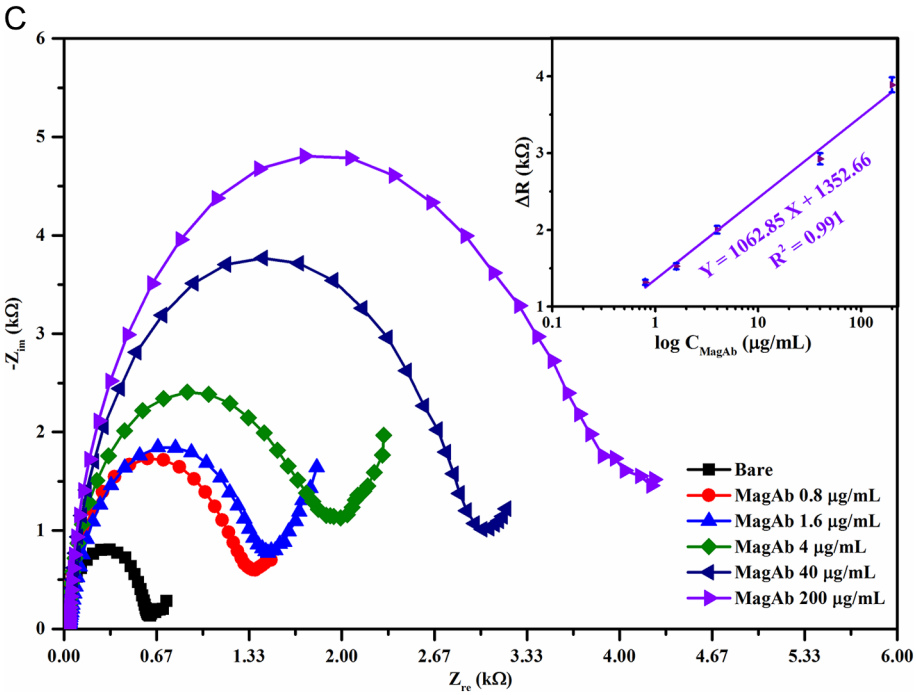


**Fig. 2.** (*continued*)

0.01 μg/mL lipopolysaccharide alone (0.055; Fig. S3A). The absorbance of the magnetosome (2 mg/mL) - antibody (200 μg/mL) complex with lipopolysaccharide (0.324) was higher than the absorbance of the antibody complex alone (0.296) and 0.01 μg/mL lipopolysaccharide alone (0.055; Fig. S3B). This absorbance difference indicated that lipopolysaccharide interacts with the magnetosome-antibody complex. A similar interaction was also observed at other concentrations of magnetosome-antibody complexes (0.8–40 μg/mL) and lipopolysaccharides.

### *3.4.2. ELISA based detection of lipopolysaccharides using magnetosome-anti-Salmonella antibody complexes*

Magnetosome (1 or 2 mg/mL) conjugated to anti-*Salmonella* antibody (0.8–200 μg/mL) were used in this assay, along with unconjugated anti-*Salmonella* antibody (0.8–200 μg/mL). A magnetosome (2 mg/mL)-antibody (4 μg/mL) complex showed good absorbance (1.791). Lower concentrations of anti-*Salmonella* antibody (1.6, 2 and 2.6 μg/mL) conjugated to 2 mg/mL magnetosome also showed good absorbance at ~0.632. In comparison, magnetosome at 1 mg/mL conjugated to anti-*Salmonella* antibody at 0.8–200 μg/mL showed lower absorbance values. The lower concentrations of magnetosome (at 1 mg/mL)-antibody (at 1.6, 2, 2.6, and 4 μg/mL) complex also showed very low absorbance (0.137). The lower concentrations of uncoupled antibody (1.6, 2, 2.6 and 4 μg/mL) also showed low absorbance (0.234). This illustrates that magnetosome-antibody complex with 2 mg/mL magnetosome and 0.8–200 μg/mL antibody detected lipopolysaccharide more efficiently than the complex with 1 mg/mL magnetosome or antibody alone (0.8–200 μg/mL; Fig. S4A). The lowest concentration of lipopolysaccharide (0.001 μg/mL) could be detected by using the complex of 2 mg/mL magnetosome and 1.6 μg/mL antibody in ELISA. Further, a marked difference in absorbance (0.447) was observed between this magnetosome-antibody (2 mg/mL/1.6 μg/mL) complex and the uncoupled antibody at 1.6 μg/mL. In the ELISA, there was an approximately 60% decrease in anti-*Salmonella* antibody usage when magnetosome was included. The graph in Fig. 3A shows the absorbance values at various antibody concentrations (0.8–200 μg/mL) without or with magnetosome (1 and 2 mg/mL), which showed a linear relationship with antibody concentration, with regression coefficients of 0.951, 0.976, and 0.963, respectively.

An ELISA was also performed using magnetosome-anti-*Salmonella* antibody complexes to detect lipopolysaccharide at different concentrations (0.001–5 μg/mL). Lipopolysaccharide at 0.001 μg/mL was detected with magnetosome (2 mg/mL)–antibody (4 μg/mL) complex which showed higher absorbance (0.534) than 4 μg/mL antibody alone (0.345). Further, the magnetosome-antibody complex could detect 0.001 μg/mL lipopolysaccharide, whereas the antibody alone could only detect 0.005 μg/mL lipopolysaccharide. Thus, the complex showed higher sensitivity than the antibody alone (Fig. S4B). The graph in Fig. 3B shows the absorbance values at various concentrations of lipopolysaccharide detected by 4 μg/mL antibody alone or in complexed with magnetosome (1 and 2 mg/mL), which showed a linear relationship, with regression coefficients of 0.967, 0.981, and 0.992, respectively.

### *3.5. Electrochemical impedance (EIS) measurement to detect lipopolysaccharide*

The bare electrode showed small semi-circle in the high-frequency range, and a straight line in the lower frequency range, with a Warburg impedance (Fig. 4A). The Warburg resistance confirms the transfer of electrons on the electrode, indicating diffusion. The $R_{CT}$ value of the anti-*Salmonella* antibody (0.8 μg/mL) was 509 Ω, whereas in the presence of lipopolysaccharide (0.01 μg/mL) the value increased two-fold to 1208 Ω (Fig. 4A; Table S4). The transfer of electrons on the electrode surface after the addition of lipopolysaccharide occurred through charge transfer rather than diffusion (Fig. 4C and D). Interaction between lipopolysaccharide (0.01 μg/mL) and the magnetosome-antibody complex (at 2 mg/mL and 0.8 μg/mL, respectively) led to a two-fold higher $R_{CT}$ value (2040 Ω) than the magnetosome-antibody complex alone (1312 Ω; Fig. 4A, Table S4).

The interaction of magnetosome-anti-*Salmonella* antibody (2 mg/mL-0.8 μg/mL) complex with various concentrations of lipopolysaccharide (0.001–0.1 μg/mL) was studied. The highest concentration of lipopolysaccharide (0.1 μg/mL) showed very high resistance, with an $R_{CT}$ value of 3254 Ω. The other concentrations of lipopolysaccharides showed concurrent decrease in $R_{CT}$ value with decreased concentration (0.05 μg/mL - 2820 Ω, 0.01 μg/mL - 2057 Ω, 0.005 μg/mL - 1483 Ω,

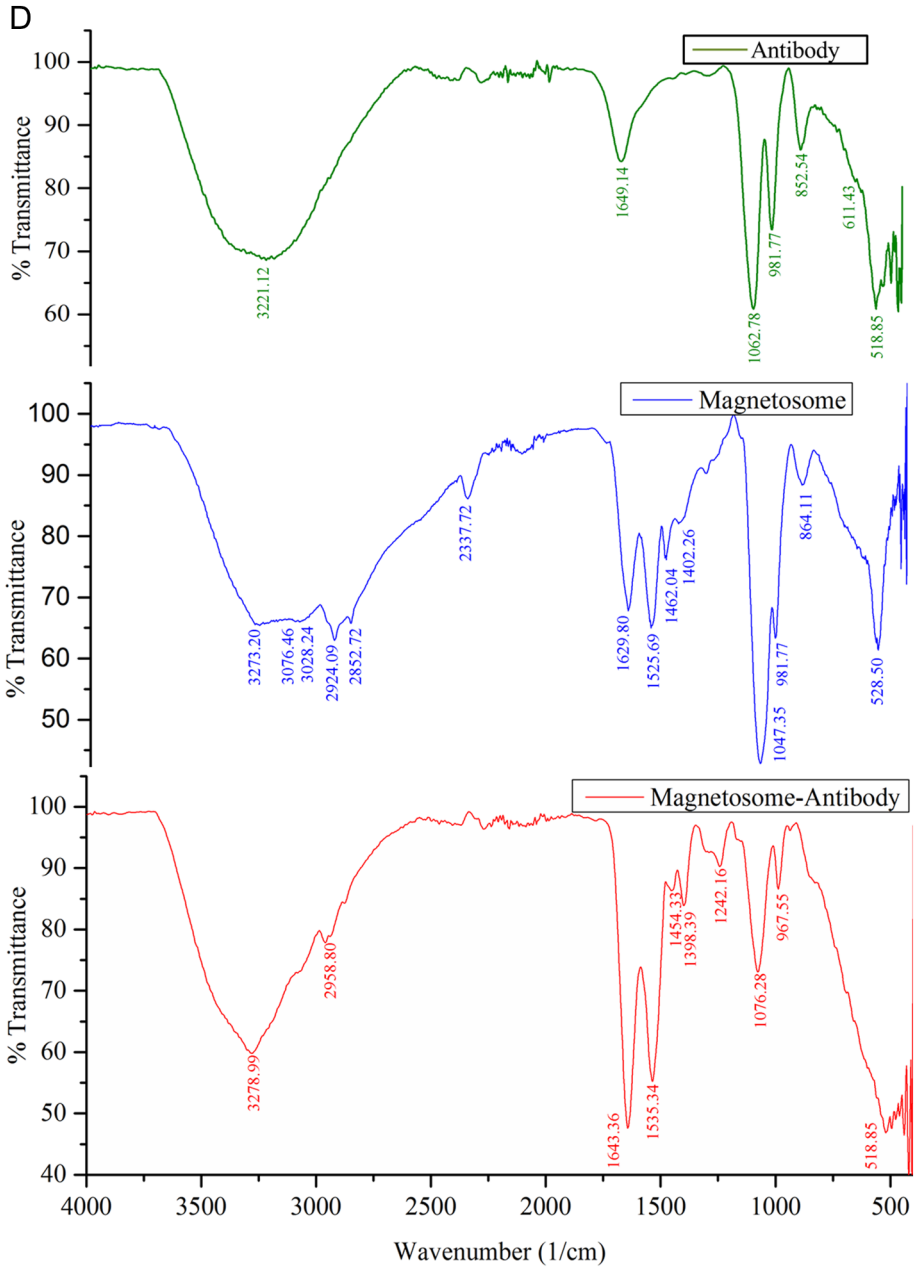


**Fig. 2.** (*continued*)

and 0.001 μg/mL - 1226 Ω) (Fig. 4B; Table S5). The calibration graph (Fig. 4B) at varying concentrations of lipopolysaccharide shows a linear relationship, with a regression coefficient of 0.960. The circuit diagram shows that the electron transfer that occurred on the surface of the electrode after lipopolysaccharide modification was due to charge transfer (Fig. 4D). These results confirmed the detection of lipopolysaccharide using the magnetosome-antibody complex.

### *3.6. Detection of lipopolysaccharide from contaminated samples using ELISA*

The magnetosome-anti-*Salmonella* antibody (2 mg/mL-0.8 μg/mL) complex was more sensitive than the antibody alone (0.8 μg/mL) for detecting the lipopolysaccharide extracted from *S. typhimurium*-infected sample (Fig. 5A). The absorbance of the magnetosome-antibody complex (1.246) was comparatively higher than that of the antibody alone (1.112) in a *S. typhimurium*-infected water sample. Similarly, the magnetosome-antibody complex (1.249) showed higher absorbance than antibody alone (0.547) in a *S. typhimurium*-infected milk sample. Uninfected water and milk samples showed a minimum reaction with the antibody and magnetosome-antibody complex. Lipopolysaccharide extracted from *S. typhimurium*-infected sample was successfully detected on an SPCE using the magnetosome-antibody (2 mg/mL-0.8 μg/mL) complex as *S. typhimurium*-infected milk and water samples showed a two-fold increase in resistance with $R_{CT}$ values of 2846 Ω (water) and 3290 Ω (milk), compared to that of the corresponding controls ($R_{CT}$ = 1648 Ω for water and 1954 Ω for milk; Fig. 5B, Table S6).

The cross-reactivity of the magnetosome-antibody complex using proteins from three other pathogens verified the specificity of the sensor. Among the four tested pathogens, the magnetosome-antibody complex showed maximum reactivity in the *S. typhimurium*-infected homogenized milk sample with $\Delta R_{CT}/R_{CT}$ of 1 Ω (Fig. 5C). The results also indicated insignificant interaction of magnetosome-antibody complex with proteins from other pathogens.

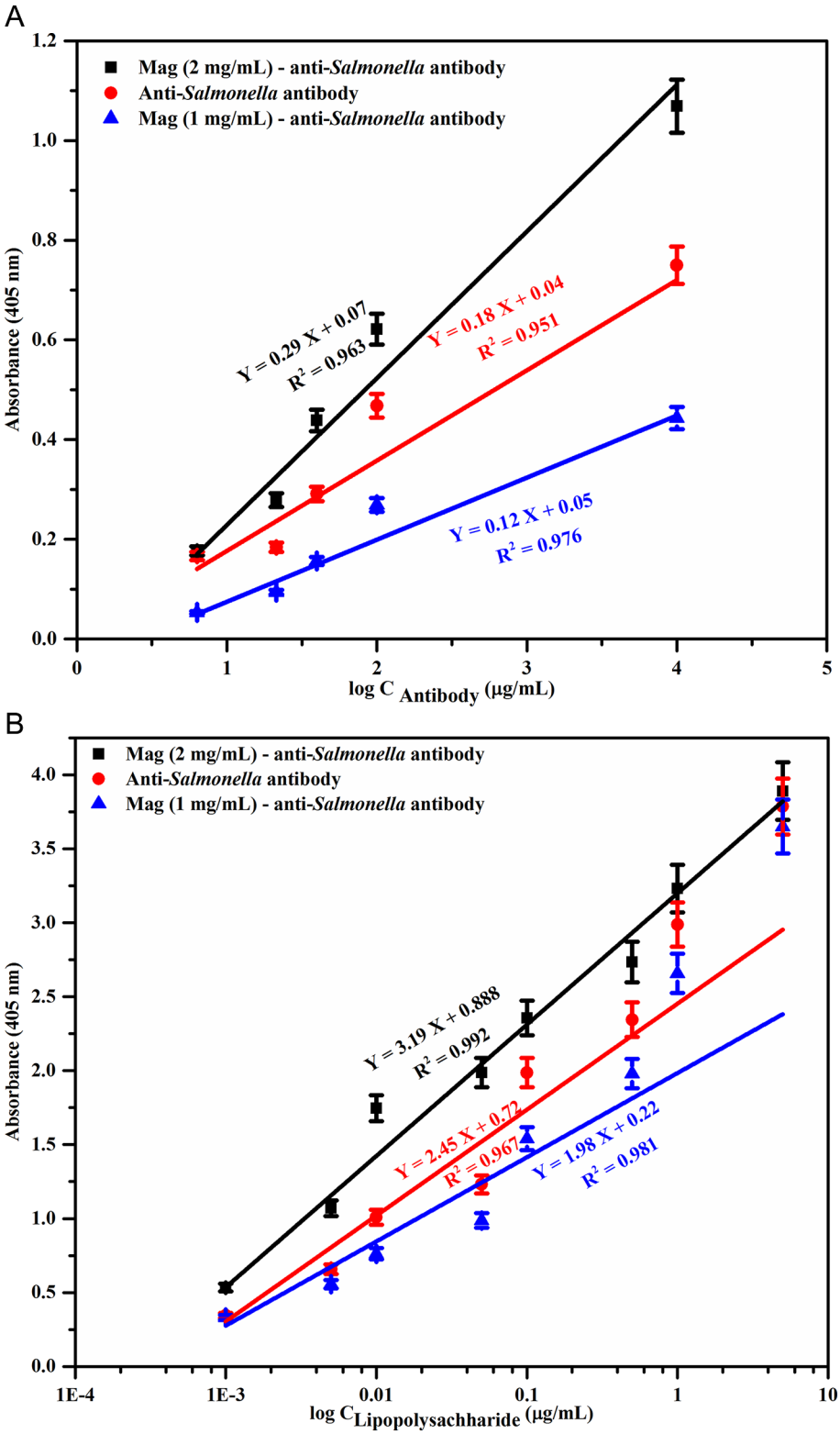


**Fig. 3.** (A): Inset: variation of absorbance with log ($C_{antibody}$). All the concentrations ranging from 0.8–200 µg/mL with 2 mg/mL concentrations of magnetosome efficiently detected the lipopolysaccharide compared to others.
(B): Inset: variation of absorbance with log ($C_{lipopolysaccharide}$). All the concentrations of lipopolysaccharide (0.001–5 µg/mL) was efficiently detected in 2 mg/mL concentration of magnetosome with antibody (0.8 µg/mL) compared to others.

### *3.7. EIS to detect Salmonella typhimurium in food samples and a capture efficiency assay*

The magnetosome-antibody (2 mg/mL-0.8 µg/mL) complex could detect *S. typhimurium* in both water and milk. The sensitivity of the technique was high, as it could detect $10^1$ CFU/mL in water and milk. The $R_{CT}$ values in water increased with increasing concentration of cells (1975, 2254, 2322, 2402, 2589, 2854, and 3017 Ω at 10-fold dilutions

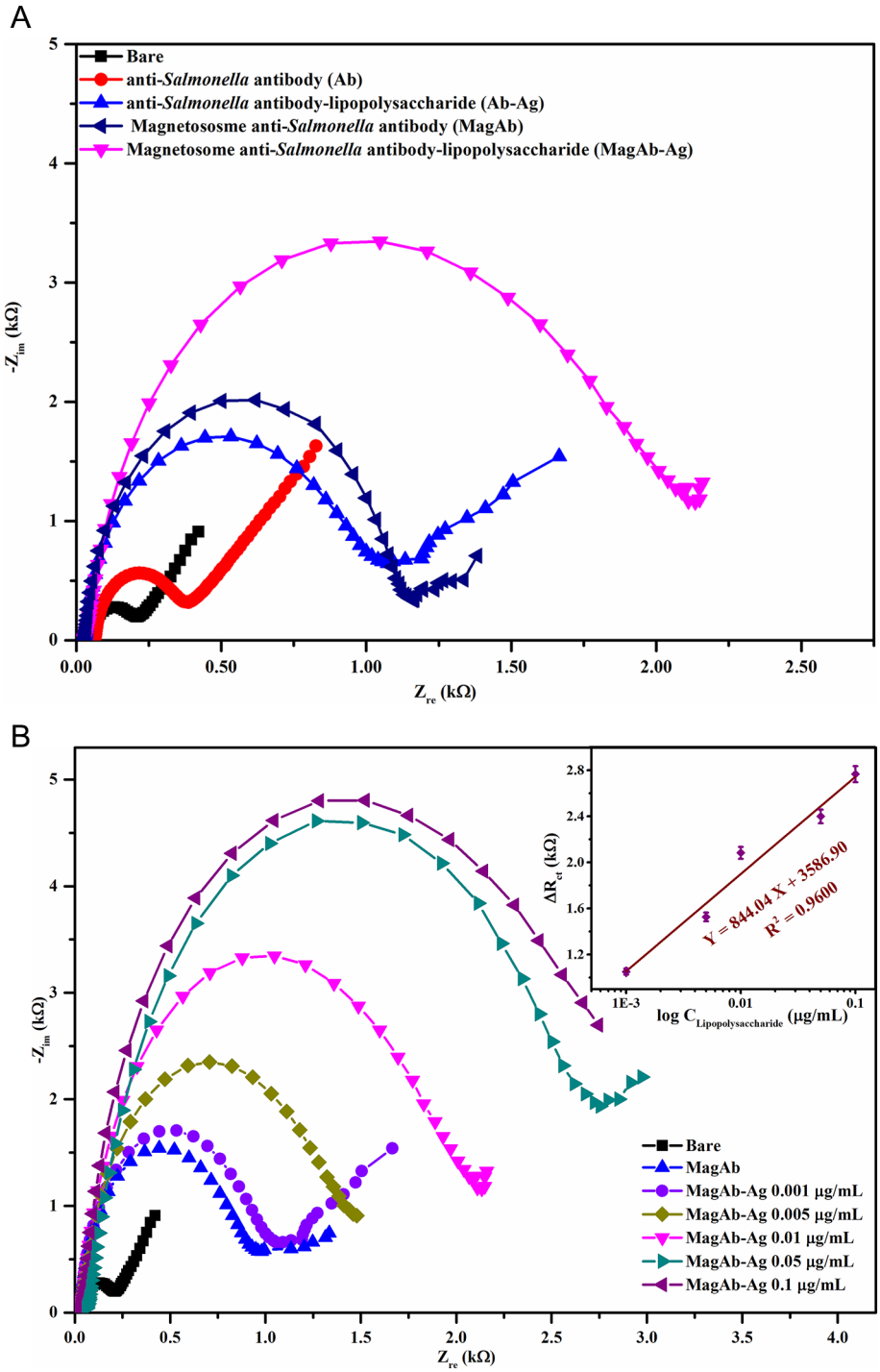


**Fig. 4.** (A): Nyquist plot for the interaction of anti-*Salmonella* antibody (0.8 μg/mL) and magnetosome (2 mg/mL)-anti-*Salmonella* antibody (0.8 μg/mL) complex with lipopolysaccharide (0.01 μg/mL).
(B): Nyquist plot for the interaction of magnetosome (2 mg/mL)-anti-*Salmonella* antibody complex (0.8 μg/mL) with various concentration of lipopolysaccharide (0.001–0.1 μg/mL) and calibration of $\Delta R_{ct}$ with log ($C_{lipopolysaccharide}$).
(C): A circuit model of electrode representing bare, (D) modification with magnetosome-anti-*Salmonella* antibody complex and lipopolysaccharide.

from $10^1$ to $10^7$ CFU/mL, respectively; Fig. 6A, Table S7). Similarly, the $R_{CT}$ values in milk were directly proportional to the increasing concentration (at 1453, 1757, 1994, 2143, 2244, 2562, and 2845 Ω, respectively; Fig. 6B, Table S8). The calibration graphs show a linear relationship between concentration and $R_{CT}$ value, with regression coefficients of 0.974 and 0.982 for water and milk respectively. The controls for water and milk both showed low resistance.

The FE-SEM analysis revealed that the magnetosome-antibody complexes were imbedded over rod shaped *S. typhimurium* (Fig. 6C). This confirms the positive interaction of magnetosome-antibody complex with *S. typhimurium*. The capture efficiency of the magnetosome-antibody complex in the milk and water samples was greater in samples with high cell counts. In milk, the capture efficiency was > 90% at all tested concentrations, whereas in water, the capture efficiency was moderate (Table S9).

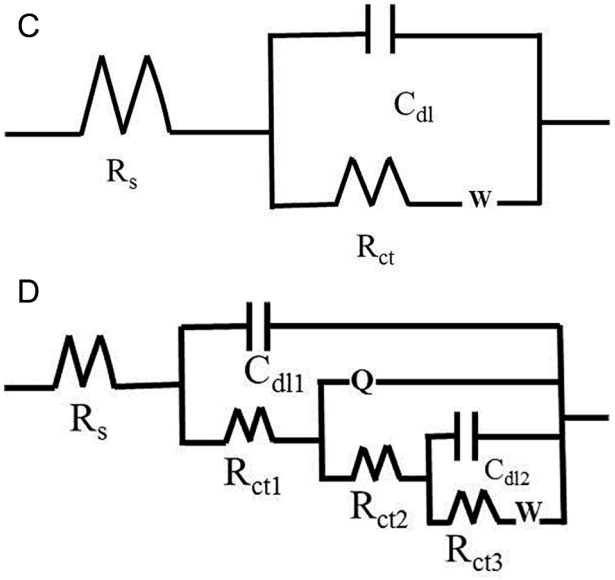


**Fig. 4.** (*continued*)

## 4. Discussion

Magnetosomes have gained the much interest among the researchers in the field of biotechnology [66]. The lipid bilayer of the magnetosome imparts a unique ability to directly bind to biomolecules [67]. However, commercial applications of magnetosome are yet to be exploited. Here, we present the development of a magnetosome-based biosensor and for the detection *S. typhimurium* lipopolysaccharide. Previous studies exploring the biotechnological application of magnetosome focused on the reported strains MSR-1, AMB-1, MS-1 and MV-1 [68–71]. In contrast, our study focused on the use of magnetosome extracted from the novel strain *Magnetospirillum* sp. RJS-1 [56].

Although nanoparticles provide a specific surface for biomolecule reactions, they have several drawbacks [72,73] mainly the instability of biomolecule attachment [74]. Thus, wide ranges of linker molecules have been implemented; however, this complicates the process and affects the biomolecule binding reactions [75–77]. In our study, we directly conjugated magnetosome to *Salmonella*-specific polyclonal antibodies which was confirmed by spectroscopy and impedimetric analysis. Direct coupling of the antibody to the magnetosome simplifies the reaction and eliminates the use of linker molecules, which significantly reduces cost and time. The magnetosome antibody conjugates were

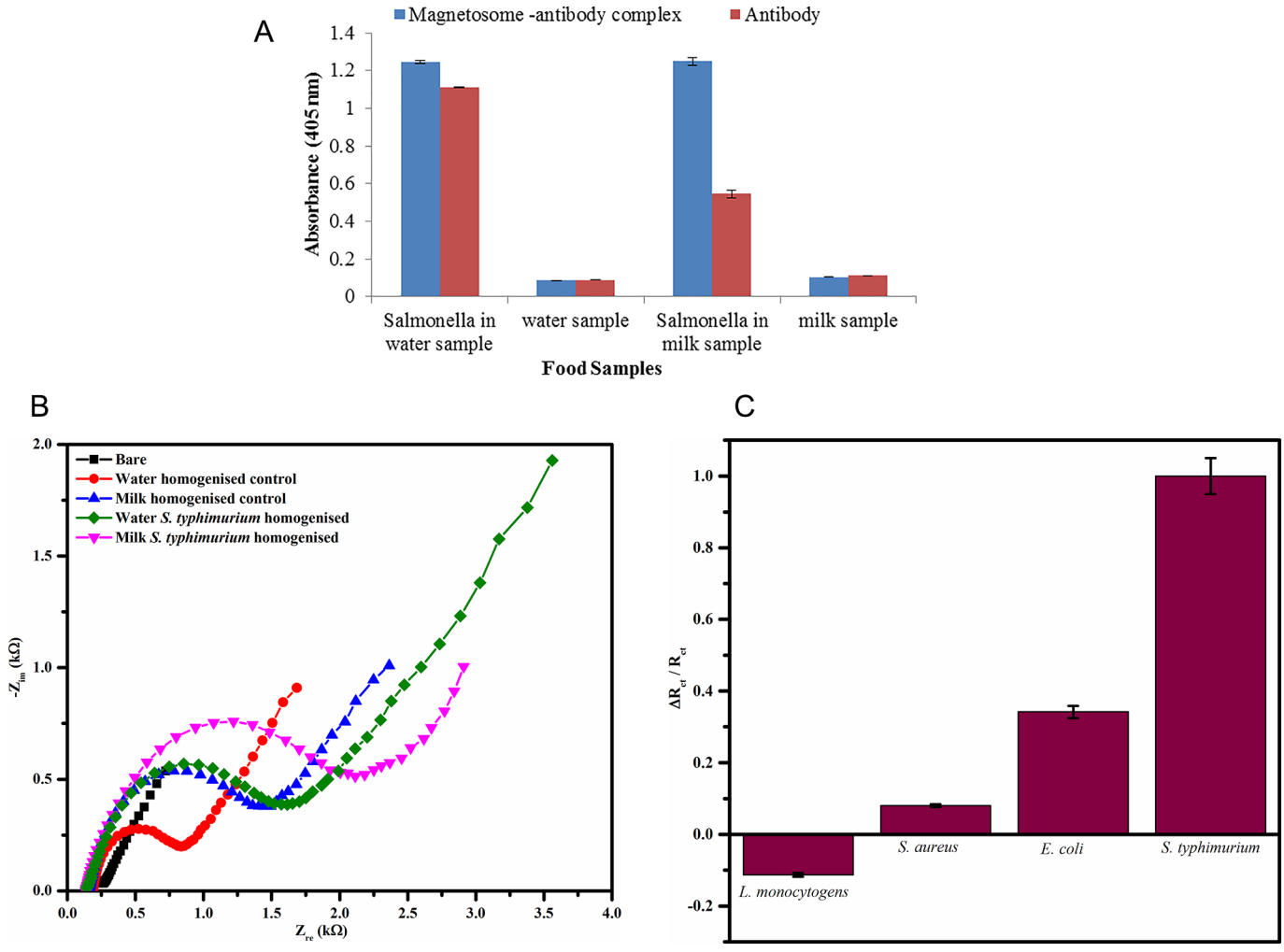


**Fig. 5.** Detection of *Salmonella typhimurium* from homogenized water and milk sample using magnetosome (2 mg/mL)-antibody (0.8 μg/mL) complex in (A) ELISA (B) EIS. (C) Cross-reactivity assay.

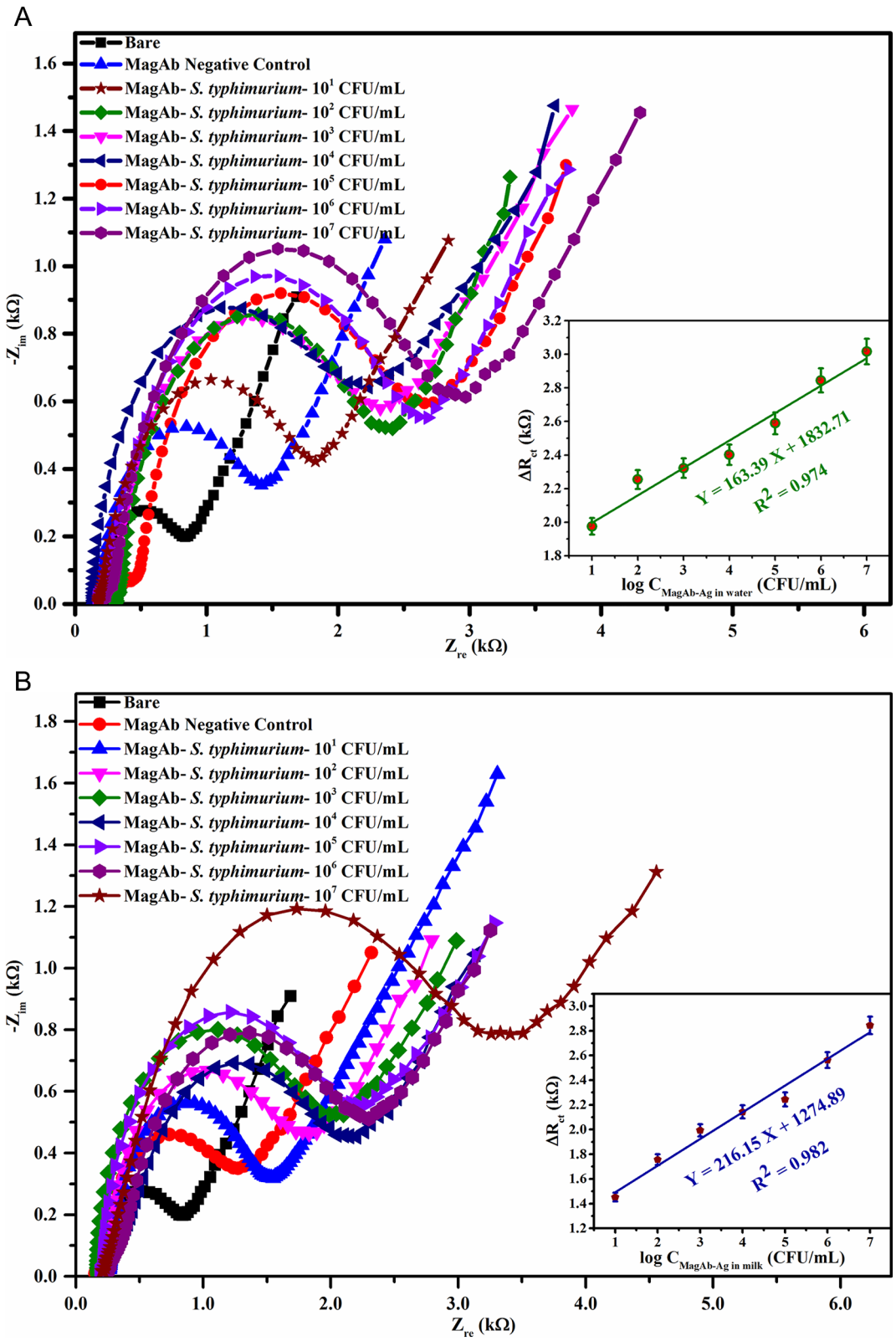


**Fig. 6.** (A): Nyquist diagrams for the interaction of magnetosome (2 mg/mL)-antibody (0.8 μg/mL) complex with various concentrations of *Salmonella typhimurium* in the water sample.
(B): Nyquist diagrams for the interaction of magnetosome (2 mg/mL)-antibody (0.8 μg/mL) complex with various concentrations of *Salmonella typhimurium* in the milk sample.
(C): FE-SEM image of *Salmonella typhimurium* interacting with the magnetosome-antibody complex in milk sample at 200 nm scale bar.

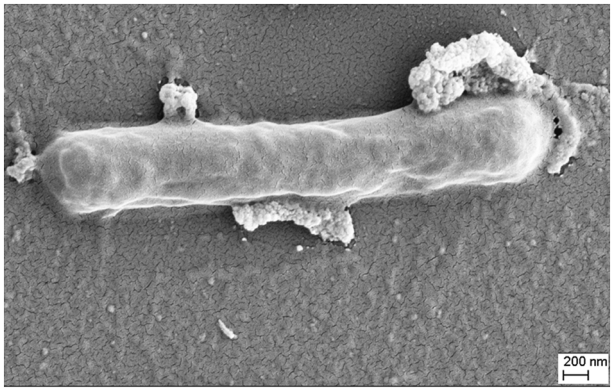


**Fig. 6.** (*continued*)

relatively stable due to negative zeta potential value [78]. Our process is a simple method that uses minimal buffer and can be completed within 24 h.

In our study, lipopolysaccharide bound to the magnetosome-anti-*Salmonella* antibody complex, which was confirmed by spectroscopy analysis. ELISA was also performed to detect lipopolysaccharide by using the magnetosome-antibody complex. The concentration of magnetosome-antibody complex required to detect lipopolysaccharide in the ELISA was reduced to 60% of the concentration of antibody required. Previous studies used higher concentrations of anti-*Salmonella* antibodies (500 μg/mL) conjugated to magnetic nanoparticles [79]. However, in the present study, magnetosome-bound anti-*Salmonella* antibody at 1.6 μg/mL was sufficient to detect lipopolysaccharide. Therefore, ours is a more cost-effective approach because the antibody concentration was considerably reduced. In addition, a lower concentration of lipopolysaccharide (0.001 μg/mL) could be detected when the magnetosome-antibody complex was employed; thereby, elevating the sensitivity of the ELISA by 50%. Lee et al. [80] developed a 1-day ELISA to detect *Salmonella*; however, the minimum concentration for detection was 1 μg/mL. The modified ELISA presented in our study is easy to perform with some alterations, and the samples can be stored for a long time without affecting the assay, offering a better alternative to the traditional assay.

Despite the demonstrated increased sensitivity of the ELISA, such magnetosome applications are restricted to the laboratory scale. Therefore, the present research focused on the development of a magnetosome-based biosensor. Biosensors are well suited for the detection of lipopolysaccharide in food samples [81,82]. To develop a magnetosome-based biosensor, a magnetosome-anti-*Salmonella* antibody complex was applied to an SPCE to detect lipopolysaccharide by EIS. In previous studies, a tedious process was required for antibody immobilization on the electrode surface, which involved the use of various chemicals and reagents [84]. In our approach, the use of magnetosome stabilizes the antibody on the surface of the working electrode by using an external magnetic field. In addition, the SPCEs are easy to handle and the need for sophisticated instrumentation is eliminated [83,85]. The antigen-antibody reaction is also well monitored on the surface of the carbon electrode [19].

The interaction of the magnetosome-antibody complex with lipopolysaccharide was verified by EIS. The increase in resistance during binding demonstrated interaction between the antibody and lipopolysaccharide in the presence of magnetosome. Further, the transfer of electrons on the surface of the modified electrode was shown to occur through charge transfer rather than diffusion. The charge transfer of electrons indicates interaction between lipopolysaccharide and the magnetosome-antibody complex. The detection of lipopolysaccharide by EIS is a rapid process that only took 4 h, unlike ELISA, which usually takes 24 h [86]. In addition, EIS requires a minimum number of reagents, with a maximum volume of 15 μL, whereas the minimum volume of antigen and antibody required for ELISA is 100 μL [87]. The graphs of the interaction of the magnetosome-antibody complex with various concentrations of lipopolysaccharide (0.001–5 μg/mL) by ELISA (0.992) and EIS (0.960) showed linearity. The minimum time required for EIS and the minimal amount of reagents used demonstrated that it is a rapid and cost-effective approach. The minimal concentration of antigen could be easily measured as an increase in resistance, which demonstrates the sensitivity of the approach.

The prospective magnetosome-based biosensor for detecting *S. typhimurium* was further tested by using food and water samples. The infected samples were homogenized, and the presence of lipopolysaccharide was confirmed by ELISA. The magnetosome (2 mg/mL) conjugated to a minimum concentration of anti-*Salmonella* antibody (0.8 μg/mL) was able to detect the extracted lipopolysaccharides. Cho and Irudayaraj [88] immobilized gold particles with a high concentration of antibody (15 μg/mL) to detect lipopolysaccharides via ELISA. Although, positive results were obtained in ELISA, the EIS detected the presence of extracted lipopolysaccharides in both water and milk within 30 min. However, the water and milk samples contained other proteins, and thus, the specificity of the magnetosome-antibody complex for infected samples were confirmed in a cross-reactivity assay. Gold nanoparticles based biosensors are costly and lagging behind in functioning than magnetic nanoparticle based biosensors [89]. Magnetosome with magnetic nature in it, proves advantageous in our study.

The developed biosensor was further used to detect *S. typhimurium* in real water and milk samples. A wide range of *Salmonella* cells ($10^1$–$10^7$ CFU/mL) were directly detected in infected water and milk within 30 min. Previous studies showed similar results, with a detection range of $10^1$ to $10^8$ CFU/mL [63,90]; however, the magnetosome-based biosensor used in our study was most rapid and simple. The FE-SEM analysis also confirmed the interaction of magnetosome-antibody complex with *S. typhimurium* in milk sample. Moreover, our magnetosome-antibody complex detection method could capture 90% of the cells from water and milk samples which validated results of our study. In future studies, this rapid, cost-effective, sensitive, and specific magnetosome-based biosensor could be further enhanced by developing miniature portable, user- friendly devices. These devices could be easily implemented on a commercial scale to directly detect pathogens in food, water, and other sources.

## 5. Conclusions

The magnetosome (2 mg/mL)-anti-*Salmonella* antibody (0.8 μg/mL) complex designed in our study was effective for lipopolysaccharide detection. The modified ELISA was more cost efficient (60%), sensitive (50%), and rapid than traditional assays. The interaction of the magnetosome-antibody complex with lipopolysaccharide was studied on a SPCE by EIS, and the minimum concentration of lipopolysaccharide detected was 0.001 μg/mL. This magnetosome-based biosensor could rapidly detect extracted lipopolysaccharide and directly detect *S. typhimurium* in water and milk within 30 min. The prototype model is rapid, cost–effective, sensitive, and specific for the detection of *S. typhimurium*. In future research, the model could be further applied on a commercial scale for the rapid detection of pathogens.

## CRediT authorship contribution statement

**Sumana Sannigrahi:** Methodology, Validation, Formal analysis, Investigation, Data curation, Writing - original draft, Writing - review & editing, Visualization. **Shiva Kumar Arumugasamy:** Software, Formal analysis, Investigation, Writing - review & editing. **Jayaraman Mathiyarasu:** Conceptualization, Formal analysis, Resources, Supervision, Project administration, Funding acquisition, Writing - review & editing. **Suthindhiran K:** Conceptualization, Validation, Resources, Data curation, Writing - review & editing, Visualization, Supervision, Project administration, Funding acquisition.

## Declaration of competing interest

The authors declare that they have no known competing financial interests or personal relationships that could have appeared to influence the work reported in this paper.

## Acknowledgements

This study has been funded by Grant-in-Aid from DBT-No. BT/PR10570/PFN/20/839/2013. We would like to thank the management of Vellore Institute of Technology and CSIR - Central Electrochemical Research Institute for providing necessary facilities to carry out this research. The authors also wish to thank Sophisticated Test and Instrumentation Centre (STIC), CUSAT, Cochin, India for TEM images.

## Data statement

Data will be made available on request.

## Appendix A. Supplementary data

Supplementary data to this article can be found online at https://doi.org/10.1016/j.msec.2020.111071.

## References

[1] B. Nielsen, D. Baggesen, F. Bager, J. Haugegaard, P. Lind, The serological response to Salmonella serovars typhimurium and infantis in experimentally infected pigs. The time course followed with an indirect anti-LPS ELISA and bacteriological examinations, Vet. Microbiol. 47 (1995) 205–218, https://doi.org/10.1016/0378-1135(95)00113-1.

[2] B. Ivanoff, M.M. Levine, P.H. Lambert, Vaccination against typhoid fever: present status, Bull. World Health Organ. 72 (1994) 957–971.

[3] T. Pang, Z.A. Bhutta, B.B. Finlay, M. Altwegg, Typhoid fever and other salmonellosis: a continuing challenge, Trends Microbiol. 3 (1995) 253–255.

[4] P.S. Mead, L. Slutsker, V. Dietz, L.F. McCaig, J.S. Bresee, C. Shapiro, P.M. Griffin, R.V. Tauxe, Food-related illness and death in the United States, Emerg. Infect. Dis. 5 (1999) 607, https://doi.org/10.3201/2Feid0505.990502.

[5] K. Nagshetty, S.T. Channappa, S.M. Gaddad, Antimicrobial susceptibility of *Salmonella typhi* in India, J Infect Dev Ctries 4 (2010) 070–073, https://doi.org/10.3855/jidc.109.

[6] C.G. Hellerqvist, B. Lindberg, S. Svensson, T. Holme, A.A. Lindberg, Structural studies on the O-specific side-chains of the cell-wall lipopolysaccharide from *Salmonella typhimurium* 395 ms, Carbohydr. Res. 8 (1968) 43–55, https://doi.org/10.1016/S0008-6215(00)81689-4.

[7] C.R. Raetz, Bacterial lipopolysaccharides: a remarkable family of bioactive macroamphiphiles. *Escherichia coli* and Salmonella, Cell. Mol. Biol. 1 (1996) 1035–1063.

[8] A.J. Baeumner, Biosensors for environmental pollutants and food contaminants, Anal. Bioanal. Chem. 377 (2003) 434–445, https://doi.org/10.1007/s00216-003-2158-9.

[9] H. Nakamura, I. Karube, Current research activity in biosensors, Anal. Bioanal. Chem. 377 (2003) 446–468, https://doi.org/10.1007/s00216-003-1947-5.

[10] F.O. Gomes, L.B. Maia, J.A. Loureiro, M.C. Pereira, C. Delerue-Matos, I. Moura, J.J. Moura, S. Morais, Biosensor for direct bioelectrocatalysis detection of nitric oxide using nitric oxide reductase incorporated in carboxylated single-walled carbon nanotubes/lipidic 3 bilayer nanocomposite, Bioelectrochemistry 127 (2019) 76–86, https://doi.org/10.1016/j.bioelechem.2019.01.010.

[11] R. Rapini, G. Marrazza, Electrochemical aptasensors for contaminants detection in food and environment: recent advances, Bioelectrochemistry 118 (2017) 47–61, https://doi.org/10.1016/j.bioelechem.2017.07.004.

[12] Y. Yi, B. Xie, T. Zhao, Z. Li, D. Stom, H. Liu, Effect of external resistance on the sensitivity of microbial fuel cell biosensor for detection of different types of pollutants, Bioelectrochemistry 125 (2019) 71–78, https://doi.org/10.1016/j.bioelechem.2018.09.003.

[13] F.A.A. Manan, W.W. Hong, J. Abdullah, N.A. Yusof, I. Ahmad, Nanocrystalline cellulose decorated quantum dots based tyrosinase biosensor for phenol determination, Mater. Sci. Eng. C. 99 (2019) 37–46, https://doi.org/10.1016/j.msec.2019.01.082.

[14] N.T. Nguyet, V.Y. Doan, N.L. Hoang, V. Van Thu, T. Trung, V.H. Pham, P.D. Tam, A label-free and highly sensitive DNA biosensor based on the core-shell structured CeO2-NR@ Ppy nanocomposite for *Salmonella* detection, Mater. Sci. Eng. C. 96 (2019) 790–797, https://doi.org/10.1016/j.msec.2018.11.059.

[15] I. Rassas, M. Braiek, A. Bonhomme, F. Bessueille, G. Rafin, H. Majdoub, N. Jaffrezic-Renault, Voltammetric glucose biosensor based on glucose oxidase encapsulation in a chitosan-kappa-carrageenan polyelectrolyte complex, Mater. Sci. Eng. C. 95 (2019) 152–159, https://doi.org/10.1016/j.msec.2018.10.078.

[16] A.G. Gehring, C.G. Crawford, R.S. Mazenko, L.J. Van Houten, J.D. Brewster, Enzyme-linked immunomagnetic electrochemical detection of *Salmonella typhimurium*, J. Immunol. Methods 195 (1996) 15–25, https://doi.org/10.1016/0022-1759(96)00076-2.

[17] E.L. Crowley, C.K. O'Sullivan, G.G. Guilbault, Increasing the sensitivity of *Listeria monocytogenes* assays: evaluation using ELISA and amperometric detection, Analyst 124 (1999) 295–299, https://doi.org/10.1039/A806875E.

[18] D. Ivnitski, E. Wilkins, H. Tien, A. Ottova, Electrochemical biosensor based on supported planar lipid bilayers for fast detection of pathogenic bacteria, Electrochem. Commun. 2 (2000) 457–460, https://doi.org/10.1016/S1388-2481(00)00060-6.

[19] Y.H. Lin, S.H. Chen, Y.C. Chuang, Y.C. Lu, T.Y. Shen, C.A. Chang, C.S. Lin, Disposable amperometric immunosensing strips fabricated by Au nanoparticles-modified screen-printed carbon electrodes for the detection of foodborne pathogen *Escherichia coli* O157: H7, Biosens. Bioelectron. 23 (2008) 1832–1837, https://doi.org/10.1016/j.bios.2008.02.030.

[20] M.B. dos Santos, S. Azevedo, J.P. Agusil, B. Prieto-Simón, C. Sporer, E. Torrents, A. Juárez, V. Teixeira, J. Samitier, Label-free ITO-based immunosensor for the detection of very low concentrations of pathogenic bacteria, Bioelectrochemistry 101 (2015) 146–152, https://doi.org/10.1016/j.bioelechem.2014.09.002.

[21] M.F. Diouani, S. Helali, I. Hafaid, W.M. Hassen, M.A. Snoussi, A. Ghram, N. Jaffrezic-Renault, A. Abdelghani, Miniaturized biosensor for avian influenza virus detection, Mater. Sci. Eng. C. 28 (2008) 580–583, https://doi.org/10.1016/j.msec.2007.10.043.

[22] M.F. Diouani, O. Ouerghi, A. Refai, K. Belgacem, C. Tlili, D. Laouini, M. Essafi, Detection of ESAT-6 by a label free miniature immuno-electrochemical biosensor as a diagnostic tool for tuberculosis, Mater. Sci. Eng. C. 74 (2017) 465–470, https://doi.org/10.1016/j.msec.2016.12.051.

[23] T. Peng-Ubol, P. Phinyocheep, P. Daniel, W. Panbangred, J.F. Pilard, G. Thouand, M.J. Durand-Thouand, Plasma-treated polyethylene film: a smart material applied for *Salmonella* Typhimurium detection, Mater. Sci. Eng. C. 32 (2012) 2641–2648, https://doi.org/10.1016/j.msec.2012.08.027.

[24] S.M. Radke, E.C. Alocilja, A high density microelectrode array biosensor for detection of *E. coli* O157: H7, Biosens. Bioelectron. 20 (2005) 1662–1667, https://doi.org/10.1016/j.bios.2004.07.021.

[25] E. Tully, S.P. Higson, R. O'Kennedy, The development of a 'labeless' immunosensor for the detection of *Listeria monocytogenes* cell surface protein, Internalin B, Biosens. Bioelectron. 23 (2008) 906–912, https://doi.org/10.1016/j.bios.2007.09.011.

[26] J. Dong, H. Zhao, M. Xu, Q. Ma, S. Ai, A label-free electrochemical impedance immunosensor based on AuNPs/PAMAM-MWCNT-Chi nanocomposite modified glassy carbon electrode for detection of *Salmonella typhimurium* in milk, Food Chem. 141 (2013) 1980–1986, https://doi.org/10.1016/j.foodchem.2013.04.098.

[27] A. Tlili, M.A. Jarboui, A. Abdelghani, D.M. Fathallah, M.A. Maaref, A novel silicon nitride biosensor for specific antibody–antigen interaction, Mater. Sci. Eng. C. 25 (2005) 490–495, https://doi.org/10.1016/j.msec.2005.02.001.

[28] E. Katz, I. Willner, Probing biomolecular interactions at conductive and semiconductive surfaces by impedance spectroscopy: routes to impedimetric immunosensors, DNA-sensors, and enzyme biosensors, Electroynalysis (N.Y.N.Y.) 15 (2003) 913–947, https://doi.org/10.1002/elan.200390114.

[29] P.D. Skottrup, M. Nicolaisen, A.F. Justesen, Towards on-site pathogen detection using antibody-based sensors, Biosens. Bioelectron. 24 (2008) 339–348, https://doi.org/10.1016/j.bios.2008.06.045.

[30] S.H. Noh, S.H. Moon, T.H. Shin, Y. Lim, J. Cheon, Recent advances of magneto-thermal capabilities of nanoparticles: from design principles to biomedical applications, Nano Today 13 (2017) 61–76, https://doi.org/10.1016/j.nantod.2017.02.006.

[31] S.R. Dafeh, P. Iranmanesh, P. Salarizadeh, Fabrication, optimization, and characterization of ultra-small superparamagnetic Fe3O4 and biocompatible Fe3O4@ ZnS core/shell magnetic nanoparticles: ready for biomedicine applications, Mater. Sci. Eng. C. 98 (2019) 205–212, https://doi.org/10.1016/j.msec.2018.12.147.

[32] S. Zhang, N. Wang, H. Yu, Y. Niu, C. Sun, Covalent attachment of glucose oxidase to an Au electrode modified with gold nanoparticles for use as glucose biosensor, Bioelectrochemistry 67 (2005) 15–22, https://doi.org/10.1016/j.bioelechem.2004.12.002.

[33] Y. Yu, Z. Chen, S. He, B. Zhang, X. Li, M. Yao, Direct electron transfer of glucose oxidase and biosensing for glucose based on PDDA-capped gold nanoparticle modified graphene/multi-walled carbon nanotubes electrode, Biosens. Bioelectron. 52 (2014) 147–152, https://doi.org/10.1016/j.bios.2013.08.043.

[34] S. Muniandy, S.J. Teh, J.N. Appaturi, K.L. Thong, C.W. Lai, F. Ibrahim, B.F. Leo, A reduced graphene oxide-titanium dioxide nanocomposite based electrochemical aptasensor for rapid and sensitive detection of *Salmonella enterica*, Bioelectrochemistry 127 (2019) 136–144, https://doi.org/10.1016/j.bioelechem.2019.02.005.

[35] N. Elahi, M. Kamali, M.H. Baghersad, B. Amini, A fluorescence Nano-biosensors immobilization on iron (MNPs) and gold (AuNPs) nanoparticles for detection of *Shigella spp*, Mater. Sci. Eng. C. 105 (2019) 110113, , https://doi.org/10.1016/j.msec.2019.110113.

[36] S. Krishnan, T. Chinnasamy, S. Veerappan, K. Senthilkumar, D. Kannaiyan, Dual labeled Ag@ SiO2 core–shell nanoparticle based optical immunosensor for sensitive detection of *E. coli*, Mater. Sci. Eng. C. 45 (2014) 337–342, https://doi.org/10.1016/j.msec.2014.09.028.

[37] S. Pakapongpan, R.P. Poo-Arporn, Self-assembly of glucose oxidase on reduced graphene oxide-magnetic nanoparticles nanocomposite-based direct electrochemistry for reagentless glucose biosensor, Mater. Sci. Eng. C. 76 (2017) 398–405, https://doi.org/10.1016/j.msec.2017.03.031.

[38] J.S. Mitchell, Y. Wu, C.J. Cook, L. Main, Sensitivity enhancement of surface

plasmon resonance biosensing of small molecules, Anal. Biochem. 343 (2005) 125–135, https://doi.org/10.1016/j.ab.2005.05.001.
[39] L. Wang, K. Wang, S. Santra, X. Zhao, L.R. Hilliard, J.E. Smith, Y. Wu, W. Tan, Watching silica nanoparticles glow in the biological world, Anal. Chem. 78 (2006) 646–654, https://doi.org/10.1021/ac0693619.
[40] M. Yang, Y. Yang, Y. Liu, G. Shen, R. Yu, Platinum nanoparticles-doped sol–gel/carbon nanotubes composite electrochemical sensors and biosensors, Biosens. Bioelectron. 21 (2006) 1125–1131, https://doi.org/10.1016/j.bios.2005.04.009.
[41] I.I. Slowing, B.G. Trewyn, S. Giri, V.Y. Lin, Mesoporous silica nanoparticles for drug delivery and biosensing applications, Adv. Funct. Mater. 17 (2007) 1225–1236, https://doi.org/10.1002/adfm.200601191.
[42] A.L. Possan, C. Menti, M. Beltrami, A.D. Santos, M. Roesch-Ely, F.P. Missell, Effect of surface roughness on performance of magnetoelastic biosensors for the detection of *Escherichia coli*, Mater. Sci. Eng. C. 58 (2016) 541–547, https://doi.org/10.1016/j.msec.2015.08.029.
[43] S.K. Banerjee, B.M. Moskowitz, Ferrimagnetic Properties of Magnetite. Magnetite Biomineralization and Magnetoreception in Organisms, Springer, Boston, MA, 1985, pp. 17–41, https://doi.org/10.1007/978-1-4613-0313-8_2.
[44] D.A. Bazylinski, A.J. Garratt-Reed, R.B. Frankel, Electron microscopic studies of magnetosomes in magnetotactic bacteria, Microsc. Res. Tech. 27 (1994) 389–401, https://doi.org/10.1002/jemt.1070270505.
[45] M. Kuhara, H. Takeyama, T. Tanaka, T. Matsunaga, Magnetic cell separation using antibody binding with protein A expressed on bacterial magnetic particles, Anal. Chem. 76 (2004) 6207–6213, https://doi.org/10.1021/ac0493727.
[46] E. Alphandéry, Y. Ding, A.T. Ngo, Z.L. Wang, L.F. Wu, M.P. Pileni, Assemblies of aligned magnetotactic bacteria and extracted magnetosomes: what is the main factor responsible for the magnetic anisotropy? ACS Nano 3 (2009) 1539–1547, https://doi.org/10.1021/nn900289n.
[47] N. Nakamura, T. Matsunaga, Highly sensitive detection of allergen using bacterial magnetic particles, Anal. Chim. Acta 281 (1993) 585–589, https://doi.org/10.1016/0003-2670(93)85018-F.
[48] R.B. Frankel, D.A. Bazylinski, D. Schüler, Biomineralization of magnetic iron minerals in bacteria, Supramol. Sci. 5 (1998) 383–390, https://doi.org/10.1016/S0968-5677(98)00036-4.
[49] A. Arakaki, H. Nakazawa, M. Nemoto, T. Mori, T. Matsunaga, Formation of magnetite by bacteria and its application, J. R. Soc. Interface 5 (2008) 977–999, https://doi.org/10.1098/rsif.2008.0170.
[50] T. Matsunaga, Genetic analysis of magnetic bacteria, Mater. Sci. Eng. C. 4 (1997) 287–289, https://doi.org/10.1016/S0928-4931(97)00012-X.
[51] H.T. Tien, A. Ottova-Leitmannova, Membrane Biophysics: As Viewed From Experimental Bilayer Lipid Membranes, 5 Elsevier, 2000.
[52] D. Schüler, R.B. Frankel, Bacterial magnetosomes: microbiology, biomineralization and biotechnological applications, Appl. Microbiol. Biotechnol. (4) (1999) 464–473, https://doi.org/10.1007/s002530051547.
[53] R. Wacker, B. Ceyhan, P. Alhorn, D. Schueler, C. Lang, C.M. Niemeyer, Magneto Immuno-PCR: a novel immunoassay based on biogenic magnetosome nanoparticles, Biochem. Biophys. Res. Commun. 357 (2007) 391–396, https://doi.org/10.1016/j.bbrc.2007.03.156.
[54] J.J. Jacob, K. Suthindhiran, Magnetotactic bacteria and magnetosomes–scope and challenges, Mater. Sci. Eng. C. 68 (2016) 919–928, https://doi.org/10.1016/j.msec.2016.07.049.
[55] L. Wu, B. Gao, F. Zhang, X. Sun, Y. Zhang, Z. Li, A novel electrochemical immunosensor based on magnetosomes for detection of staphylococcal enterotoxin B in milk, Talanta 106 (2013) 360–366, https://doi.org/10.1016/j.talanta.2012.12.053.
[56] T. Revathy, J.J. Jacob, M.A. Jayasri, K. Suthindhiran, Isolation and characterization of *Magnetospirillum* from saline lagoon, World J. Microbiol. Biotechnol. 32 (2016) 109, https://doi.org/10.1007/s11274-016-2075-7.
[57] R.E. Hungate, The anaerobic mesophilic cellulolytic bacteria, Bacteriol. Rev. 14 (1950) 1–49.
[58] R.P. Blakemore, D. Maratea, R.S. Wolfe, Isolation and pure culture of a freshwater magnetic spirillum in chemically defined medium, J. Bacteriol. 140 (1979) 720–729.
[59] E. Alphandéry, F. Guyot, I. Chebbi, Preparation of chains of magnetosomes, isolated from *Magnetospirillum magneticum* strain AMB-1 magnetotactic bacteria, yielding efficient treatment of tumors using magnetic hyperthermia, Int. J. Pharm. 434 (2012) 444–452, https://doi.org/10.1016/j.ijpharm.2012.06,015.
[60] M.A. Woo, M. Kim, J. Jung, K. Park, T. Seo, H. Park, A novel colorimetric immunoassay utilizing the peroxidase mimicking activity of magnetic nanoparticles, Int. J. Mol. Sci. 14 (2013) 9999–10014, https://doi.org/10.3390/ijms14059999.
[61] H. Wu, Y. Zuo, C. Cui, W. Yang, H. Ma, X. Wang, Rapid quantitative detection of *Brucella melitensis* by a label-free impedance immunosensor based on a gold nanoparticle-modified screen-printed carbon electrode, Sensors 13 (2013) 8551–8563, https://doi.org/10.3390/s130708551.
[62] M. Varshney, L. Yang, X.L. Su, Y. Li, Magnetic nanoparticle-antibody conjugates for the separation of *Escherichia coli* O157: H7 in ground beef, J. Food Prot. 68 (2005) 1804–1811, https://doi.org/10.4315/0362-028X-68.9.1804.
[63] M. Varshney, Y. Li, Interdigitated array microelectrode based impedance biosensor coupled with magnetic nanoparticle–antibody conjugates for detection of *Escherichia coli* O157: H7 in food samples, Biosens. Bioelectron. 22 (2007) 2408–2414, https://doi.org/10.1016/j.bios.2006.08.030.
[64] E.B. Setterington, E.C. Alocilja, Electrochemical biosensor for rapid and sensitive detection of magnetically extracted bacterial pathogens, Biosensors 2 (2012) 15–31, https://doi.org/10.3390/bios2010015.
[65] E. Sheikhzadeh, M. CHamsaz, A.P.F. Turner, E.W.H. Jager, V. Beni, Label-free impedimetric biosensor for *Salmonella Typhimurium* detection based on poly [pyrrole-co-3-carboxyl-pyrrole] copolymer supported aptamer, Biosens. Bioelectron. 80 (2016) 194–200, https://doi.org/10.1016/j.bios.2016.01.057.
[66] L. Yan, X. Yue, S. Zhang, P. Chen, Z. Xu, Y. Li, H. Li, Biocompatibility evaluation of magnetosomes formed by *Acidithiobacillus ferrooxidans*, Mater. Sci. Eng. C. 32 (2012) 1802–1807, https://doi.org/10.1016/j.msec.2012.04.062.
[67] Y.A. Gorby, T.J. Beveridge, R.P. Blakemore, Characterization of the bacterial magnetosome membrane, J. Bacteriol. 170 (1988) 834–841, https://doi.org/10.1128/jb.170.2.834-841.1988.
[68] B.M. Moskowitz, R.B. Frankel, D.A. Bazylinski, H.W. Jannasch, D.R. Lovley, A comparison of magnetite particles produced anaerobically by magnetotactic and dissimilatory iron-reducing bacteria, Geophys. Res. Lett. 16 (1989) 665–668, https://doi.org/10.1029/GL016i007p00665.
[69] C.D. Yang, H. Takeyama, T. Tanaka, T. Matsunaga, Effects of growth medium composition, iron sources and atmospheric oxygen concentrations on production of luciferase-bacterial magnetic particle complex by a recombinant *Magnetospirillum magneticum* AMB-1, Enzym. Microb. Technol. 29 (2001) 13–19, https://doi.org/10.1016/S0141-0229(01)00343-X.
[70] B.L. Dubbels, A.A. DiSpirito, J.D. Morton, J.D. Semrau, J.N.E. Neto, D.A. Bazylinski, Evidence for a copper-dependent iron transport system in the marine, magnetotactic bacterium strain MV-1, Microbiology 150 (2004) 2931–2945, https://doi.org/10.1099/mic.0.27233-0.
[71] J.B. Sun, F. Zhao, T. Tang, W. Jiang, J.S. Tian, Y. Li, J.L. Li, High-yield growth and magnetosome formation by *Magnetospirillum gryphiswaldense* MSR-1 in an oxygen-controlled fermentor supplied solely with air, Appl. Microbiol. Biotechnol. 79 (2008) 389, https://doi.org/10.1007/s00253-008-1453-y.
[72] X. Luo, A. Morrin, A.J. Killard, M.R. Smyth, Application of nanoparticles in electrochemical sensors and biosensors, Electroanalysis 18 (2006) 319–326, https://doi.org/10.1002/elan.200503415.
[73] B. Tian, X. Liao, P. Svedlindh, M. Strömberg, E. Wetterskog, Ferromagnetic resonance biosensor for homogeneous and volumetric detection of DNA, ACS Sens 3 (2018) 1093–1101, https://doi.org/10.1021/acssensors.8b00048.
[74] S.M. Hussain, K.L. Hess, J.M. Gearhart, K.T. Geiss, J.J. Schlager, In vitro toxicity of nanoparticles in BRL 3A rat liver cells, Toxicol. in Vitro 19 (2005) 975–983, https://doi.org/10.1016/j.tiv.2005.06.034.
[75] E. Galoppini, Linkers for anchoring sensitizers to semiconductor nanoparticles, Coord. Chem. Rev. 248 (2004) 1283–1297, https://doi.org/10.1016/j.ccr.2004.03.016.
[76] O.V. Salata, Applications of nanoparticles in biology and medicine, J Nanobiotechnology 2 (2004) 3, https://doi.org/10.1186/1477-3155-2-3.
[77] H.S. Kim, I.H. Cho, S.M. Seo, J.W. Jeon, S.H. Paek, In situ immuno-magnetic concentration-based biosensor systems for the rapid detection of *Listeria monocytogenes*, Mater. Sci. Eng. C 32 (2012) 160–166, https://doi.org/10.1016/j.msec.2011.10.012.
[78] J. Xu, J. Hu, L. Liu, L. Li, X. Wang, H. Zhang, W. Jiang, J. Tian, Y. Li, J. Li, Surface expression of protein A on magnetosomes and capture of pathogenic bacteria by magnetosome/antibody complexes, Front. Microbiol. 5 (2014) 136, https://doi.org/10.3389/fmicb.2014.00136.
[79] S.P. Ravindranath, L.J. Mauer, C. Deb-Roy, J. Irudayaraj, Biofunctionalized magnetic nanoparticle integrated mid-infrared pathogen sensor for food matrixes, Anal. Chem. 81 (2009) 2840–2846, https://doi.org/10.1021/ac802158y.
[80] H.A. Lee, G.M. Wyatt, S. Bramham, M.R. Morgan, Enzyme-linked immunosorbent assay for *Salmonella typhimurium* in food: feasibility of 1-day Salmonella detection, Appl. Environ. Microbiol. 56 (1990) 1541–1546.
[81] F.C. Tenover, Diagnostic deoxyribonucleic acid probes for infectious diseases, Clin. Microbiol. Rev. 1 (1988) 82–101, https://doi.org/10.1128/CMR.1.1.82.
[82] P. Arora, A. Sindhu, N. Dilbaghi, A. Chaudhury, Biosensors as innovative tools for the detection of food borne pathogens, Biosens. Bioelectron. 28 (2011) 1–12, https://doi.org/10.1016/j.bios.2011.06.002.
[83] A.A. Karyakin, G.V. Presnova, M.Y. Rubtsova, A.M. Egorov, Oriented immobilization of antibodies onto the gold surfaces via their native thiol groups, Anal. Chem. 72 (2000) 3805–3811, https://doi.org/10.1021/ac9907890.
[84] J. Wang, B. Tian, V.B. Nascimento, L. Angnes, Performance of screen-printed carbon electrodes fabricated from different carbon inks, Electrochim. Acta 43 (1998) 3459–3465, https://doi.org/10.1016/S0013-4686(98)00092-9.
[85] I. Gandouzi, M. Tertis, A. Cernat, A. Bakhrouf, M. Coros, S. Pruneanu, C. Cristea, Sensitive detection of pyoverdine with an electrochemical sensor based on electrochemically generated graphene functionalized with gold nanoparticles, Bioelectrochemistry 120 (2018) 94–103, https://doi.org/10.1016/j.bioelechem.2017.11.014.
[86] S.X. Leng, J.E. McElhaney, J.D. Walston, D. Xie, N.S. Fedarko, G.A. Kuchel, ELISA and multiplex technologies for cytokine measurement in inflammation and aging research, J. Gerontol. A Biol. Sci. Med. Sci. 63 (2008) 879–884, https://doi.org/10.1093/gerona/63.8.879.
[87] M.F. Clark, A.N. Adams, J., Characteristics of the microplate method of enzyme-linked immunosorbent assay for the detection of plant viruses, J Gen. Virol. 34 (1977) 475–483, https://doi.org/10.1099/0022-1317-34-3-475.
[88] I.H. Cho, J. Irudayaraj, In-situ immuno-gold nanoparticle network ELISA biosensors for pathogen detection, Int. J. Food Microbiol. 164 (2013) 70–75, https://doi.org/10.1016/j.ijfoodmicro.2013.02.025.
[89] W. Nouira, A. Maaref, H. Elaissari, F. Vocanson, M. Siadat, N. Jaffrezic-Renault, Comparative study of conductometric glucose biosensor based on gold and on magnetic nanoparticles, Mater. Sci. Eng. C 33 (2013) 298–303, https://doi.org/10.1016/j.msec.2012.08.043.
[90] H. Kaur, M. Shorie, M. Sharma, A.K. Ganguli, P. Sabherwal, Bridged Rebar Graphene functionalized aptasensor for pathogenic *E. coli O78: K80: H11* detection, Biosens. Bioelectron. 98 (2017) 486–493, https://doi.org/10.1016/j.bios.2017.07.

004.

**Sumana Sannigrahi** is pursuing Ph.D. from Vellore Institute of Technology (VIT), India. She is a recipient of Senior Research Fellowship from Department of Biotechnology, Government of India. She received her Masters of Sciences in Applied Microbiology from VIT in 2015 and Bachelor of Sciences (Hons) in Microbiology and Microbial Technology from Sam Higginbottom University of Agriculture, Technology and Sciences in 2013. Her research focuses on development of magnetosome based electrochemical biosensor for the detection of various food and aquatic pathogens.

**Shiva Kumar Arumugasamy** received Masters of Technology in Industrial Biotechnology from the SASTRA University in 2016 and Bachelor of Technology in Biotechnology from Mepco Schlenk Engineering College in 2014. He joined as a Junior Research Fellow in CSIR-Central Electrochemical Research Institute during 2016 and learnt about the electrochemical sensing techniques. His research focuses on nanostructured materials, particularly carbon nanomaterials for applications in sensor and electrochemical energy storage.

**Jayaraman Mathiyarasu** is a Senior Principal Scientist at CSIR-Central Electrochemical Research Institute, India. He pursued his post-doctoral fellowship in the area of chemical sciences – Novel materials and Biosensors at the Department of Material science, The Angstrom Laboratory, Uppsala University, Sweden. He had visited Kurt-Schwabe Institute for sensor and Measuring Technology, Meinsberg, Germany for an Indo-German project entitled “Design and development of electrochemical sensors for human healthcare applications”. He had been the head for developing a NPK based sensor development for the agricultural usage; using fundamental sciences and modern technologies. His research focuses on the fundamental investigations concerning electrochemical (bio) sensors based on integrated micro and nano-structures and nanocomposites.

**Suthindhiran K** is an Assistant Professor (Senior) at Vellore Institute of Technology (VIT), India. He received his Ph.D. from VIT in 2010. He is a recipient of Young Scientist award from SERB-DST, Govt of India. He has completed three projects funded by DBT and DST. His lab is first to report the diversity and characterization of marine magnetotactic bacteria from India. His research focuses on diversity and exploitation of marine microorganisms including magnetotactic bacteria and actinomycetes. His lab is working on exploiting the magnetosomes for various applications including biosensor development, drug delivery, waste management, water purification etc.